Performance analysis of new liquid cooling topology and its impact on data centres

Mohamad Hnayno, Ali Chehade, Henryk Klaba, Hadrien Bauduin, Guillaume Polidori, Chadi Maalouf

Performance analysis of new liquid cooling topology and its impact on data centres

Mohamad HNAYNO [(1)], Ali CHEHADE [(1)], Henryk KLABA [(1)], Hadrien BAUDUIN [(1)], Guillaume POLIDORI [(2)], Chadi MAALOUF [(2)]

[1] OVHcloud, 155 Avenue Georges Hannart, 59170 Croix, France.

[2] MATIM, University of Reims Champagne-Ardenne, 51100 Reims, France.

Abstract

A large amount of the energy consumed by data centres is related to the cooling demand. The use of optimised liquid cooling technology enables one to increase the water inlet temperature and the water temperature difference of a data centre. Accordingly, the energy consumption of the data centre infrastructure can be reduced by appropriately utilising free cooling available on-site. This paper presents an experimental investigation and performance analysis conducted on a novel liquid-cooled topology deployed within OVHcloud data centres. A rack cooling system based on a combination of close-coupled cooling and direct-to-chip cooling is presented. The experimental setup used comprised five information-technology racks with operational servers under different temperature profiles (15 K and 20 K) for two thermal conditions (27 °C and 35 °C). The results indicated a repartitioning of thermal load absorption between close coupled cooling and direct-to-chip cooling to approximately 56% and 44 %, respectively. Thereby, air was still necessary as a coolant for the data centre. A temperature difference was validated for all the information technology racks, whereas the 20 K temperature-difference profile was validated with the proposed new rear-door heat exchanger (RDHX) configuration. In addition, a performance analysis was performed on a data centre of 600 kW cooled with this topology for three heat rejection systems (mechanical cooling system using chillers, indirect free cooling with evaporative cooling, and hybrid chillers with intelligent dry coolers) under four climatic conditions. Indirect free cooling combined with an evaporative cooling system showed optimal energy savings. A reduction in annual power consumption by 89 % was achieved compared with the mechanical cooling system at four locations where data centres were located. The cooling partial power usage effectiveness of data centre was reduced by at least 16 % with respect to mechanical cooling. An increase in the temperature difference of the information technology racks from 15 K to 20 K caused a reduction in the water usage effectiveness of the data centre by at least 40 %. An increase in the temperature of the cold water supplied to the data centre by 5 K caused a reduction in water usage effectiveness and annual water consumption by at least 30 % and 47%, respectively.

Keywords: Data centre cooling, free cooling, liquid cooling, energy, heat transfer

Corresponding authors: mohamad.hnayno@ovhcloud.com, ali.chehade@ovhcloud.com, chadi.maalouf@univ-reims.fr

1. Introduction

Cloud computing and data centres (DCs) have become valuable parts of our lives because of many vital internet-scale facilities such as internet-wide search, email services, and artificial intelligence. The use of DCs has been increasing exponentially. Consequently, their energy consumption and environmental impact have become progressively more significant. The energy costs of DCs increase by 1 % every five years, as presented by Buyya et al. [1]. The most recent statistical studies presented by Kamiya et Kvarnström [2] estimated that DCs worldwide consumed approximately 200 TW-h in 2018. This accounted for 1 % of the electricity consumption worldwide. The electricity consumption in a DC repartition shows that 44 % is consumed by the DC information technology (IT) equipment; 40 % by the cooling system; and 16 % by the electrical power distribution, UPS, lighting, and other service-building usage [3]. The cooling systems in DCs account for the largest portion of the total electricity consumption after IT equipment. Thus, there is a vital need to address environmental issues by ensuring the use of cooling systems with low power consumption for DCs. The power usage effectiveness (PUE) is a measure of the efficiency with which a DC consumes power. It is defined as the ratio of the total DC power consumption to the computing-equipment power consumption. The ideal PUE is 1.0.

It is high priority to reduce the power consumption of DC cooling systems through optimised thermal management techniques [4,5]. Two key cooling-solutions have been developed over the past years: air cooling and liquid cooling. Air-cooled DCs have several constraints [6,7]. The convective heat transfer coefficient of air is low because of its poor thermal properties. Furthermore, the difficulty of achieving an appropriate airflow control system and the absence of a system to achieve it in certain DCs presented by Dai et al. [8] resulted in the mixing of heat dissipated from IT equipment with the cold air supplied. This caused hot spots around and inside the racks. The circulation of hot air that exhausts from the rack outlet into the cold air stream supplied to rack inlets by a computer room air handler (CRAH) causes IT equipment to underperform, malfunction, or fail completely. The DC environment needs to be overcooled to cool these hot spots efficiently. However, certain servers may still receive inadequate cooling. Thus, the mixing of warm and cool airstreams, reliance on air as a heat transfer medium, and power consumption of cooling hardware cause air cooling systems to be ineffective. Liquid-cooled water systems can support high-intensity power and have a wide range of advantages.

At present, two main water liquid cooling techniques are used to cool DCs: close-coupled cooling and direct liquid cooling (see Table 1). Thermal resistance can be reduced dramatically using water liquid cooling solutions. Water has a heat-carrying capacity (approximately 3.3 times higher than that of air). CPUs and GPUs are the equipment on a server that consumes the most energy. Thus, liquid cooling via direct-to-chip cooling has been demonstrated to be an efficient technology because the water temperature returning from IT equipment of DCs is significantly higher than that typically observed in closely coupled cooling systems [9]. Zimmermann et al. [10] demonstrated that a differential temperature of 15 K between the chip and coolant was sufficient for chip cooling using water as a coolant in the IBM BladeCenter Chassis. Ljungdahl et al. verified that the coolant temperature has a direct impact on energy savings and cooling efficiency [11]. Coles et Greenberg [12] demonstrated that direct-to-chip cooling achieves a significant decrease in the total DC site energy-consumption (by 14–20 %).

Liquid cooling solutions	Description

Close coupled cooling	In-row Cooling [7]	• Row-based air conditioning units are installed inside the rack rows. • Airflows interact with the ambient room environment (Open-loop solution). • Typical inlet water temperature = 12–23 °C
	In-rack Cooling [13]	• The cooling system is combined with the server rack, and both are sealed completely. • No interaction with the ambient room environment (Closed-loop solution) • Typical inlet water temperature = 12–23 °C
	Rear Door Heat Exchanger [14,15]	• This type of solution is based on a combination of fans and a finned heat exchanger installed on the rear side of racks. • Airflows interact with the ambient room environment (Open-loop solution). • Typical inlet water temperature = 12–23 °C
Direct-to-chip cooling	Cold plates [16]	• A heat sink with micro-channels (cold plates) is in direct contact with IT components of the DC, such as CPUs and GPUs. Here, the water flowing across absorbs chip energy. • Typical inlet water temperature 27–45 °C

Table 1. Data-centre water liquid cooling solutions.

Recently, many researchers focused on the evaluation of optimised cooling technologies for energy savings and reduction of environmental impact. Zhang et al. [17] performed a comprehensive literature review of the cooling technologies for DCs. They concluded that a combination of multiple cooling technologies including direct-to-chip liquid cooling could be a future trend to further improve the energy efficiency of DCs. It was also indicated that the use of these energy-saving cooling technologies could help achieve average energy-savings of up to 50% compared with the conventional mechanical cooling. Udakeri et al. [18] indicated that liquid cooling and air cooling could be highly efficient when combined as a hybrid cooling strategy for DCs.

The DC market is oriented towards cloud computing, which involves more hard disks and RAMs. In this case, full cooling via cold plates is not feasible, and standard air-cooling solutions would still be required. A combination of close-coupled cooling (rear-door heat exchanger (RDHX)) and direct-to-chip cooling could be used. The rear side of a server rack is equipped with an RDHX. This eliminates the need to separate the hot/cold aisle [15]. The output water from the RDHX is reused as inlet water for the direct-to-chip liquid cooling system. Therefore, a higher DC water temperature difference (ΔT) can be achieved. This enables more extensive heat reuse [19] or the capability to reject this heat to the atmosphere with a dry cooler. This, in turn, eliminates the need for a cooling tower or chiller plant in most climates [20]. The workload of heat rejection systems used to evacuate heat to the external environment can be reduced significantly by appropriately utilising on-site available free cooling [21–23]. Evaporative cooling (EC) can be used as a pre-cooler in environments where the ambient temperatures of dry coolers are higher than the temperature of the liquid cooling supplied [24–26].

Different evaporative cooling systems can be employed to cool the inlet air [27]. These include evaporative cooling pads, which have been demonstrated to be effective [28,29].

This work focused on an experimental study to develop and validate a novel cooling topology for IT racks that is based on liquid cooling deployed within OVHcloud DCs. The paper is structured into six sections. Section 2 describes the cooling system topology. Section 3 presents an experimental bench designed and constructed to study and characterise this cooling topology at the rack level through tests conducted on five racks equipped with different profiles of IT equipment. In addition, the section describes tests performed on different configurations of RDHX to determine the best configuration to operate the DC under two thermal conditions (TC-27 °C and TC-35 °C) while preventing overheating, throttling, and equipment damage. Section 4 describes the integration of this cooling topology within a DC of 600 kW and its coupling with three heat-rejection systems (a mechanical cooling system using chillers, indirect free cooling with evaporative cooling, and hybrid chillers with integrated intelligent dry coolers) under four climatic conditions. Section 5 describes an investigation of the impact of the water-temperature profile in terms of partial power usage effectiveness and water usage effectiveness for a DC cooled with indirect free cooling using an EC pad through two approaches: rack temperature difference (Section 5.1) and increase in DC water inlet temperature (Section 5.2). Finally, in Section 6, the conclusion outlines the important results of this study.

2. Cooling system topology

OVHcloud is a French-based cloud computing company that offers VPS-and OpenStack-based public clouds. Their DCs are cooled via a liquid cooling system using an indirect free cooling technique (IFC). The technique is based on heat recovery from the servers using water pumped by a pumping substation (PSS) to direct chip heat sinks (also called water blocks (WBs)) and heat exchangers placed inside racks.

Figure 1 shows the scales of the key OVHcloud cooling system bricks. Four orders of magnitude are presented in decreasing order: heat rejection system (dry cooler) > PSS > rack RDHX and cooling distribution unit (CDU) > server WB. Cold water is pumped to the rack using PSS, heated by the rack's IT equipment, and cooled again by dry coolers installed outside the DC.

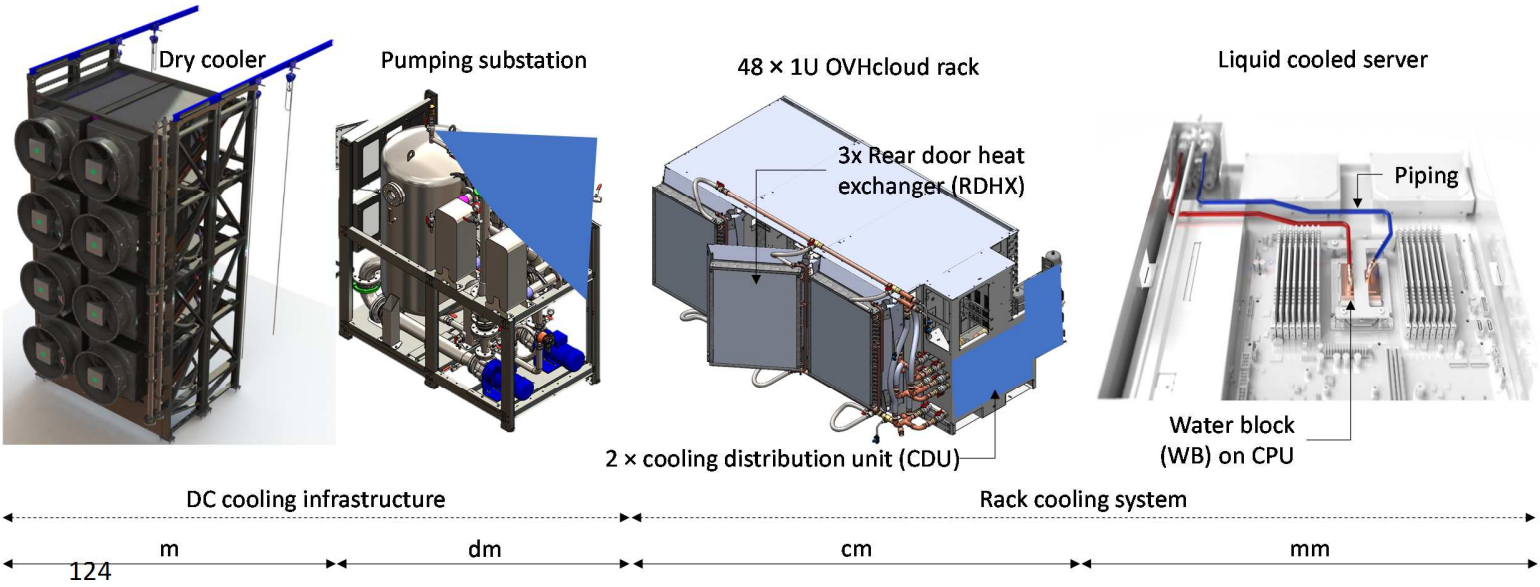

Figure 1. Scale of the cooling system studied.

Figure 2(a) shows the main elements of the system: the rack cooling system, PSS, and dry cooler. The rack cooling system is based on a combination of air and liquid cooling. It consists of RDHEXs and WBs with air/water cooling capacity (AC/WC). The water temperature is to be maintained at 27 °C for maintaining the inlet air temperature of the server and the inlet water temperature of the WB at 30 °C and 40 °C, respectively. Moisture condensation inside the DCs is prevented by operating these at the recommended temperature and humidity levels. The condensation that occurs inside IT equipment of servers causes short circuits, thereby risking the entire DC operation. Furthermore, condensation promotes corrosion and limits the lifetime of IT equipment. Table 2 lists the recommended temperature levels inside the OVHcloud DCs. The preferable temperature level is between 20 and 35 °C (green area), wherein condensation and IT equipment overheating risks are zero. The orange area includes two ranges based on the risk characteristic: 15–20 °C (where condensation is likely) and 35–40 °C (where the lifetime of IT equipment can be impacted). The DCs must be prevented from operating in the orange area. Operation in the red areas (< 15 °C and > 40 °C) is prohibited to prevent condensation and overheating risks, respectively.

Green utilisation area	Orange utilisation area	Red utilisation area
20 °C < T < 35 °C	15 °C < T < 20 °C 35 °C < T < 40 °C	T < 15 °C and T > 40 °C

Table 2. Conditions of indoor ambient temperature of DC for operating OVHcloud IT racks.

The rack current cooling system is based on a temperature difference of 15 K between the inlet and outlet of the water manifolds. As shown in Figure 2(a), water enters the RDHX at 27 °C and exits at 33 °C after absorbing the heat generated by the air-cooled IT equipment. Then, it passes through the CDU's Plate Heat Exchanger (PHEX). Finally, it recovers the heat absorbed by the WBs and exits the rack at 42 °C. Accordingly, the heat rejection system must cool the water from 42 °C to 27 °C.

An RDHX is a combination of fans and a finned heat exchanger installed on the rear side of the racks (see Figure 2(c)). The IT equipment apart from CPUs and GPUs are cooled by the RDHX. Each rack contains three rear doors. Each door is mounted on an ensemble of 16 servers called a console. Each door has 12 ebm-papst fans [1] (nominal electrical power of 4.6 W and maximal rotation speed of 3300 rpm). The fans of the rear door suck cold air from the rack's front cold side to cool the IT equipment on the servers, such as motherboards, RAM, and hard disks. The air flowing through the servers crosses the RDHX and is cooled again. Accordingly, the hot aisle is contained completely inside the rack, with both circulation aisles in front and behind the rack being cold.

The CPUs and GPUs are liquid-cooled using direct-to-chip cold plates with water as the coolant. The cold plate is called WB. It is a heat sink with channels (see Figure 2(d)), where water flows across and absorbs chip energy. WBs are fed with cold water by CDUs integrated inside the rack via a piping network. Two CDUs are installed in parallel to ensure redundant water pumping. The CDU is composed of a pump (maximum electrical power = 60 W) and plate heat exchanger (PHEX). The facility water entering the rack flows directly through the three RDHXs that cool the hot air. Then, it flows through the CDUs of the rack.

The PSS ensures the pumping of water to the racks. It is designed with a water storage tank and two redundant pumps to maximise the system availability. It provides up to 650 kW of cooling capacity to support up to 65 racks with a 10 kW load density. In addition, it contains two PHEXs for heat recovery and additional backup cooling system options. It has a small footprint of 2000 × 1000 mm. Thereby, it can be deployed conveniently irrespective of whether it is positioned next to the IT enclosures or outside the DC.

The dry coolers (or dry cooling towers) shown in Figure 2(b) play an important role in the DC cooling systems. External air is used to cool the liquid pumped around different cooling components installed in the DC without applying a refrigeration process. Depending on the external climatic conditions, dry coolers are used alternatively to cool the water supplied to the fan coils. Two types of dry coolers are used: a SlideIN cooling tower and V-shaped dry coolers (see Figure 2(b)). The SlideIN cooling tower is composed of four finned heat exchangers and eight ebm-papst AxiBlade variable-speed fans [30] (maximum electrical power of 2880 W each, and maximum rotation speed of 1000 rpm). A V-shaped dry cooler is a light-structure dry cooler composed of two finned heat exchangers and four fans (identical to those of the SlideIN cooling tower). That is, a SlideIN cooling tower is equivalent in cooling capacity to two V-shaped dry coolers.

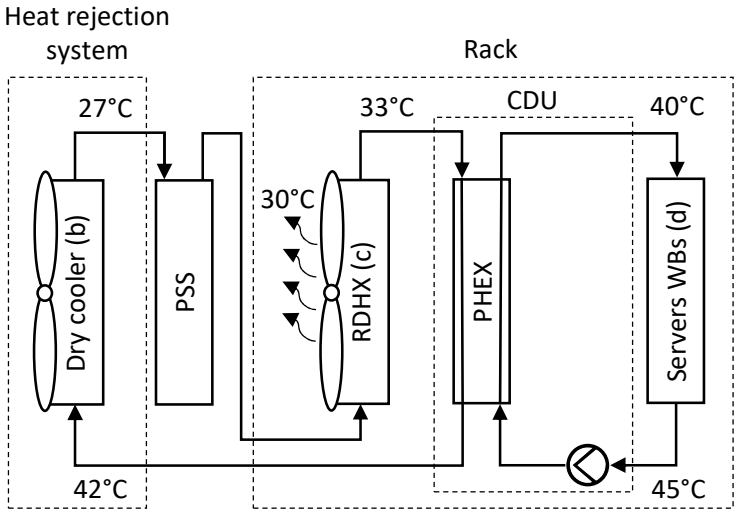

(a)

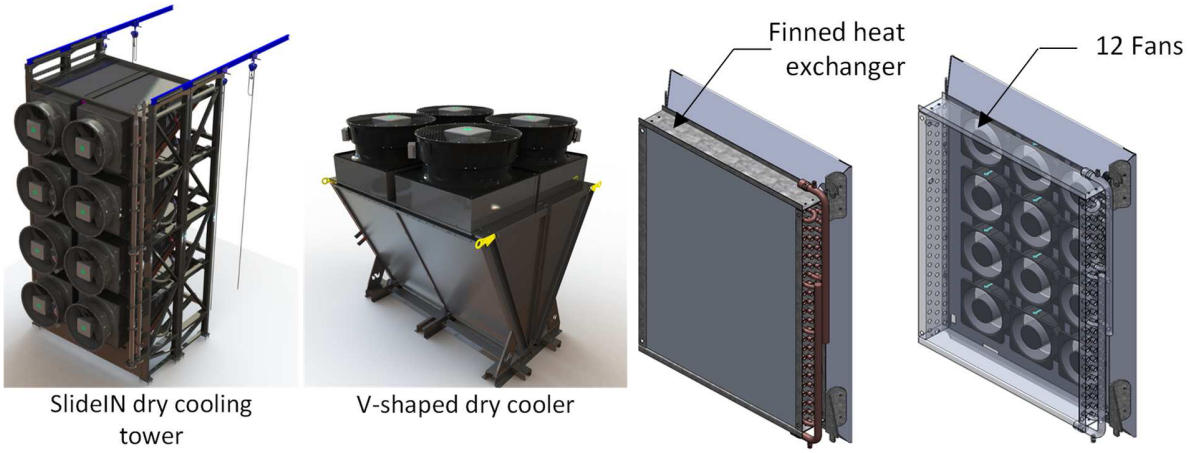

(b) (c)

(d)

Figure 2. (a) Global OVHcloud cooling system topology; (b) Different types of dry coolers; (c) Rear Door Heat Exchanger (RDHX); (d) Different types of WB-channel geometries.

3. Experimental investigation of rack level

An increase in the temperature difference in the racks causes a decrease in the flow rate of water supplied per rack. Thus, an increase in the temperature difference permits a higher heat load per pumping unit for an equivalent PSS hydraulic capacity. The dry cooler performance is likely to be enhanced significantly because water would enter higher levels, whereas fans and EC water consumption per IT kW would be reduced. Accordingly, the footprint (kW/m^2), DC infrastructure capital expenditure (CAPEX), DC operating expense (OPEX), PUE, and water usage effectiveness (WUE) would increase significantly when the heat load per PSS and dry cooler is higher. An alternative temperature profile (to that presented in Figure 2(a)) was studied. Here, the temperature difference increases from 15 K to 20 K, water flow rate increases marginally, and dry-cooler cooling capacity attains 600 kW rather than 400 kW. In this case, water enters the RDHX at a temperature of 27 °C and exits at 35 °C. It absorbs the heat generated by the air-cooled IT equipment, passes through the CDU while recovering the heat dissipated by the WBs, and exits the rack at 47 °C (see Figure 3). Accordingly, the water would be cooled from 47 °C to 27 °C using a dry cooler. A rack test bench was designed and constructed within OVHcloud Experimental DC in Croix-France to validate the direct impact of temperature difference (15 K and 20 K) on operational IT racks.

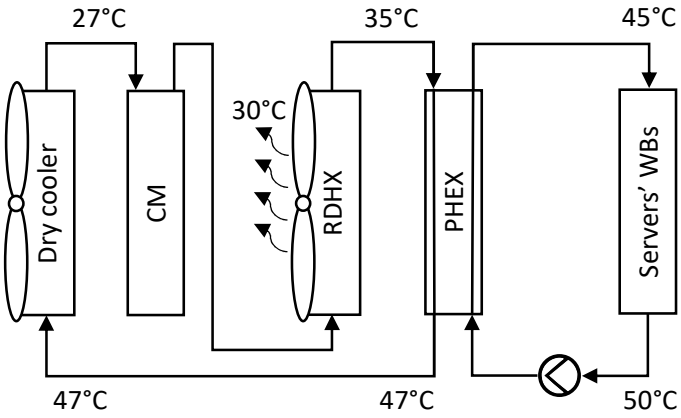

Figure 3. Topology of 20 K cooling system

3.1. Experimental setup

Figure 4(a) shows the rack test bench. A climatic chamber characterised by an insulated 20 ft maritime container was used to control the boundary conditions (ambient temperature and relative humidity) of the tested rack.

Figure 4(c) shows the hydraulic circuit of the climatic chamber. Two PSS are used: PSS-2 is the main DC PSS, and PSS1 is connected to it via a high-accuracy solenoid valve to supply water to the rack test bench. The solenoid valve was equipped with a temperature probe installed at the climatic chamber water inlet to ensure smooth regulation of the supplied temperature. Figure 4(d) shows the distribution of sensors in the system. A thermocouple was installed inside the climatic chamber to measure the

global air temperature. The internal and external wall temperatures of the climatic chamber were measured using several thermocouples installed on the walls, as well as the external ambient temperature. The system heat load and leakage were estimated accordingly. The temperature, pressure, differential pressure, and flow rate sensors were located at various positions including the inlet and outlet of each component (RDHX, PHEX, and WB servers). The details of the sensors are specified in Appendix A. It provides a detailed description of their location, suppliers, and measurement range.

The heat load is estimated as follows:

$$Q = \dot{m}\, Cp\, \Delta T \tag{1}$$

where $\dot{m}$ (kg/s) is the water flow rate, Cp (kJ/kg/°C) is the specific heat of water, and ΔT (°C) is the water temperature difference in the circuit.

The absolute pressure sensors, differential pressure sensors, thermocouples, and flow rate sensor were calibrated by comparing the response measured by each component to those measured by high-precision sensor probes. The uncertainties were evaluated using the method described by Kline and McClintock [31]. For example, the uncertainty of the thermal heat load was evaluated by

$$\frac{\Delta Q}{Q} = \sqrt{\left(\frac{\Delta \dot{m}}{\dot{m}}\right)^2 + \left(\frac{\Delta T_1}{T_2 - T_1}\right)^2 + \left(\frac{\Delta T_2}{T_2 - T_1}\right)^2} \tag{2}$$

where Δ signifies the uncertainty. T_1 and T_2 are the inlet and outlet temperatures, respectively.

Table 3 shows the uncertainties for different parameters involved in the measurements.

Parameter	Uncertainty
Temperature, $\boldsymbol{T}$ (°C)	±0.210 °C
Pressure, $\boldsymbol{P}$ (Pa)	±0.5 %
Differential pressure, $\Delta\boldsymbol{P}$ (Pa)	±0.25 %
Flow rate, $\dot{\boldsymbol{m}}$ (l/min)	±4 ml/min
Relative humidity, *RH* (%)	±2 %
Heat load, $\boldsymbol{Q}$ (W)	±1.4 %
Locations and distances (m)	±1 %
Response time (s)	±5 %

Table 3. Uncertainties for different parameters involved in the experimental tests.

The temperature sensors were type-K thermocouples with an accuracy of ±0.210 °C after the calibration process. The National Instruments data acquisition system NI cDAQ-9174 is a compact DAQ system. It was used to record all the temperatures, pressures, and flow rates throughout each experimental test (see Figure 4(b)). Then, the data were read, processed, and stored using a program running in LabView with a frequency of one measure per second [32]. In addition, the solenoid valve was controlled remotely by a Carel controller.

236

237

238 (a) (b)

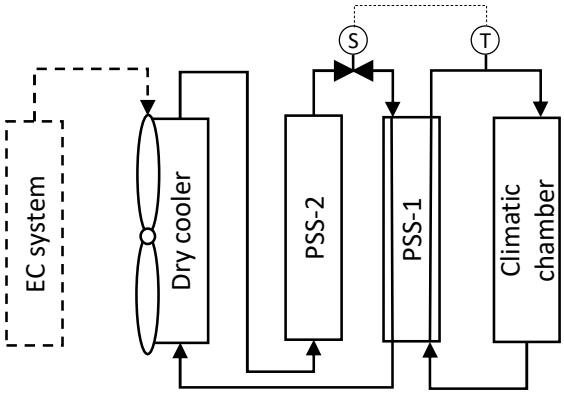

(c)

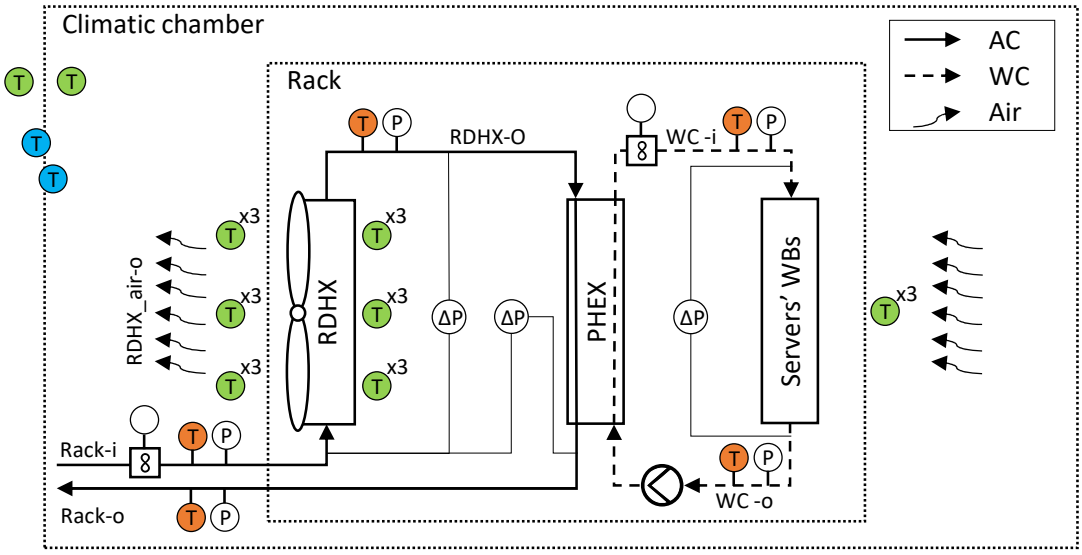

(d)

Figure 4. (a) Rack test bench; (b) Acquisition system; (c) and (d) Schematic representation of test facility and experimental setup, respectively.

Before starting the tests, the experimental loop including the rack AC and WC circuits was filled completely with water. Then, air was vented from high points to ensure that the entire circuit was free of air. The rack-supplied flow rate was adjusted manually depending on the required rack load and temperature difference. The water temperature supplied to the rack was controlled via the solenoid valve to attain the boundary conditions effectively. Moreover, the WC flow rate was adjusted directly in the CDUs. A flexible I/O (fio) script was used to stress the memory components of servers such as hard disks. CPUs and RAMs were stressed in conjunction using a script that allocates a quantity of RAM to each logical core of the CPUs to be used by a memtester process. Forty eight and 24 servers were stressed while testing 1U servers and 2U servers, respectively. Different temperature measurements of the intelligent platform management interface (IPMI) on the servers were also collected. Different IT equipment such as CPUs, GPUs, RAMs, and motherboards were analysed during each test. Other tools such as the Intel® Performance Counter Monitor and AMD uProf were used to assess the stability of server performance under different thermal conditions applied.

Tests were conducted to analyse the impact of water conditions (temperature differences of 15 and 20 K, and the water inlet temperature) on the performance of the racks. Globally, IT racks within OVHcloud DCs operate under the nominal thermal conditions of 27 °C (TC-27). First, a 15 kW rack composed of 24 × 2U servers (Rack -1) was considered under two thermal conditions (inlet water temperatures of 27 °C and 35 °C). Moreover, six RDHXs configurations having a higher cooling power corresponding to different numbers of rows and circuits (named A, B, C, D, E, and F; A is the most frequently used in OVHcloud DCs with a temperature difference of 15 K) were considered. The RDHXs have an equal surface area with a fixed fin thickness and spacing. Their tube size and fin spacing are the minimum that can be achieved with respect to each console's power for 12 fans and its fabrication technology. Additional rows per RDHX enhance the heat exchange area and heat transfer coefficient. This reduces the pinch and increases the air pressure drop and thereby, affects the rack's thermal performance as the airflow rate is reduced significantly. This, in turn, affects the turbulence and heat transfer efficiency to cause rack overheating. Thus, a combination of optimal rows and circuits is required to optimise the performance. Referring to Table 2 and to prevent DC and rack overheating, the RDHX pinch was set below a limit value ($Pinch_{\max}$) of 7 K. The RDHX power should be increased if this value exceeds the operating conditions. RDHX pinch is defined as

$$Pinch = T_{RDHX\_air-o} - T_{Rack-i} \quad (3)$$

where T_{RDHX_air-o} and T_{Rack-i} are the outlet air temperature of RDHX and inlet water temperature of rack, respectively.

3.2. Results and discussion

Table 4 shows the performance of Rack-1 under temperature differences of 15 K and 20 K for the six RDHX configurations. For RDHX A, the rack was validated under a temperature difference of 15 K. This was because its pinch is below the maximal value, whereas it exceeds the limit value at 20 K. For other

RDHX configurations and under TC-35, the rack behaviour was satisfactory and did not display overheating, throttling, or equipment damage. In addition, the rack was operated with significantly high performance without reduction in the CPU frequencies or memory bandwidth throughout the 2 h of each test.

AC/WC (%)	Condition	RDHX	T_{Rack-i} (°C)	T_{Rack-o} (°C)	ΔT (K)	Pinch (K)
54/46	TC-27	A	27.74	42.49	14.75	5.98
55/45	TC-27	A	27.84	47.93	20.09	8.53
57/43	TC-35	A	34.89	54.60	19.71	8.34
56/44	TC-35	B	35.80	56.60	20.80	3.42
57/43	TC-35	C	35.05	55.08	20.03	4.93
57/43	TC-35	D	35.05	55.97	20.92	4.01
57/43	TC-35	E	35.20	56	20.8	3.98
57/43	TC-35	F	34.78	55.11	20.33	3.89

Table 4. Thermal hydraulic behaviour of Rack-1.

Table 4 also lists the values of the ratio of air cooling capacity to water cooling capacity (percentage) within the rack. RDHX A is generally used with an AC/WC ratio of 30/70 % for old server profiles, wherein CPUs account for a substantial portion of the electrical consumption. With new server profiles filled with RAMs and hard disks, tests were switched to incremented row values (configurations B, C, D, E, and F). This ensured higher AC capacities. Thus, the AC/WC ratio of 30/70 % was no longer valid. Equilibrium was observed with an optimal pinch of 3.42 K in the RDHX B configuration for an AC/WC ratio of 56/44 %. These results show that air is still required as a coolant in addition to a water-cooling solution in cloud computing applications.

Figure 5 shows the transient thermal behaviour of the rack using RDHX B under TC-27. Initially, the rack was in standby mode. When the fio and/or memtester scripts were launched at t = 9500 s, the rack's water circuit temperature started to increase to achieve thermal equilibrium after 1 h of operation. The inlet ($T_{WC\ -i}$) and outlet ($T_{WC\ -o}$) temperatures were stabilised at 43.6 and 47.1 °C, respectively. Furthermore, the rack's water inlet ($T_{Rack\ -i}$) and outlet ($T_{Rack\ -o}$) temperatures were stabilised at 27.4 and 46.8 °C, respectively. The RDHX air outlet temperature ($T_{RDHX\ \_air-o}$) was stabilised at 32 °C. The servers showed stable and satisfactory results for all their components (RAMs, CPUs, and hard disks).

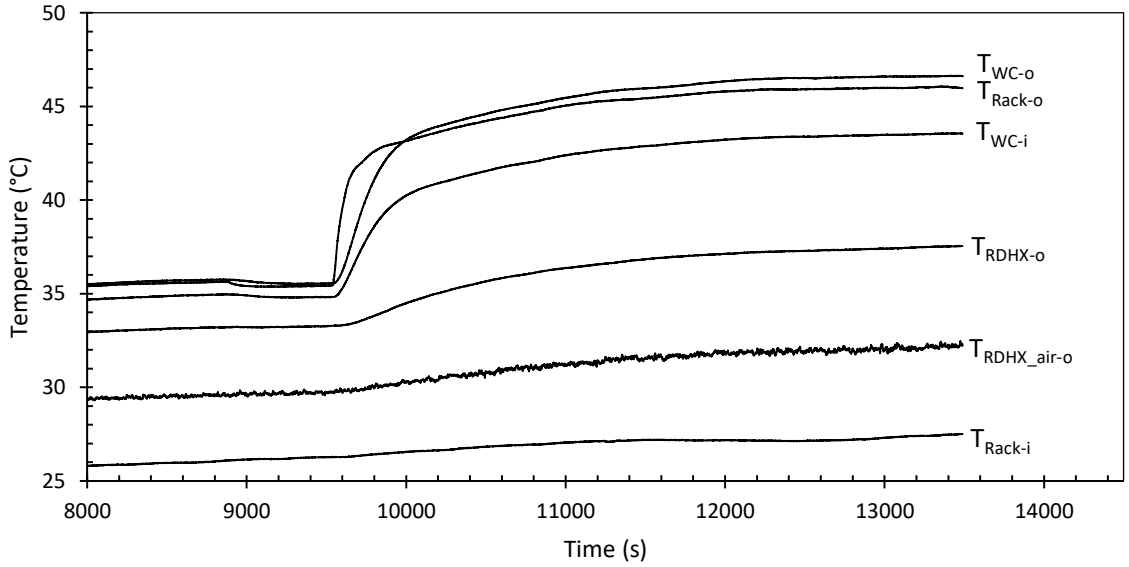

Figure 5. Transient thermal behaviour of Rack-1 using RDHX B under nominal condition (TC-27).

Work conducted on Rack-1 was repeated on four additional racks representative of the ones observed in the worldwide market to examine their performance with RDHX B. Table 5 shows the performance of the five racks under an inlet water temperature of 35 °C (TC-35) and a water temperature difference of 20 K. All the racks showed an unbalanced AC/WC ratio between 45/55 % and 58/42 %. The exception was Rack-5 (which contained additional water-cooled GPUs) with a ratio of 37/63 %.

Rack	Q (kW)	AC/WC (%)	T_{Rack-i} (°C)	T_{Rack-o} (°C)	ΔT (K)	Pinch (K)
1	15.28	56/44	35.80	56.60	20.80	3.42
2	20.66	54/46	35.35	54.39	19.04	3.84
3	13.47	45/55	35.20	54.94	19.74	3.55
4	14.19	58/42	34.96	54.81	19.85	4.48
5	27.86	37/63	34.84	56.65	21.80	4.86

Table 5. Behaviour of OVHcloud IT racks under inlet water temperature of rack of 35 °C.

The results showed that a temperature difference profile of 20 K was ensured for all the IT racks with different electrical powers. Thereby, an identical water outlet temperature was attained for all the racks. This enables convenient deployment within the DC infrastructure. With a high-water inlet temperature to the DC (up to 35 °C), condensation risk is eliminated and a long lifetime of IT equipment is insured. Besides, a 20 K temperature difference leads to a high-water outlet temperature from the DC making the free cooling solution more effective and enhancing energy saving.

This liquid cooling system was demonstrated to be efficient with a 20 K temperature-difference profile. The next section presents an analysis of the impact of this temperature difference on DC performance, and its comparison with the 15 K profile using three heat rejection systems under four climatic conditions.

4. Coupling of the new topology with different heat rejection systems

Different heat rejection systems could be used to discharge the heat of a DC to the environment. In this section, an energy analysis of three cooling systems is presented (mechanical cooling system with chillers, indirect free cooling, and hybrid chillers with integrated intelligent dry coolers). The objective is to demonstrate that the IFC can achieve optimal energy savings.

A mechanical cooling (MC) concept includes a chiller to transfer DC heat to the outdoors with a PSS, which circulates hot water from the DC to a PHEX thermally linked to the chiller (see Figure 6(a)). Water from the DC is cooled using a chiller equipped with a pumping system that circuits the glycol water between the chiller and PHEX. The chiller is installed on a secondary circuit to protect it from the high temperatures provided by the DC, which causes high-pressure build-up. The compressor, condenser fans, and pump are the active components of the chiller and consume energy. However, the high electricity consumption of the chiller compressors causes chilled-water systems to incur the highest capital cost of DC power.

Indirect free cooling (IFC) systems are driven by circulating cold water directly to cool a DC. The IFC concept involves the use of dry coolers as a heat rejection system with the DC isolated completely from its ambience. The principle of heat transfer from the coolant and its discharge to the environment is realised by air-to-water finned heat exchangers. When the sum of the outside air temperature and heat exchanger pinch exceeds the cold-water temperature to be returned to the DC, an EC system is employed to precool the outside air before cooling the fins (see Figure 6(b)).

A hybrid system is a combination of the MC and IFC systems (MC + IFC), as shown in Figure 6(c). It operates in two modes based on the outside temperature. The system operates under the MC mode at high outside temperatures. At low outside temperatures, the chiller is bypassed using a three-way valve, and the system operates in the IFC mode. This enables the DC to utilise free cooling.

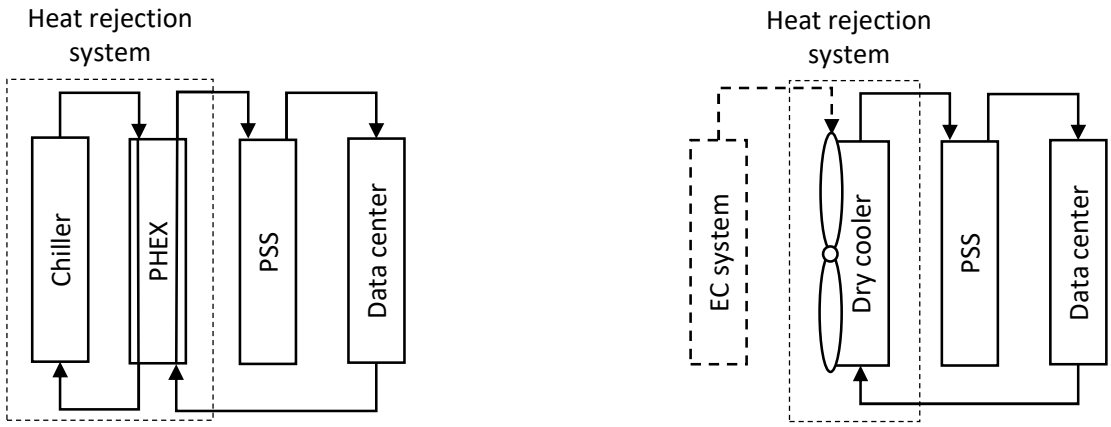

(a) (b)

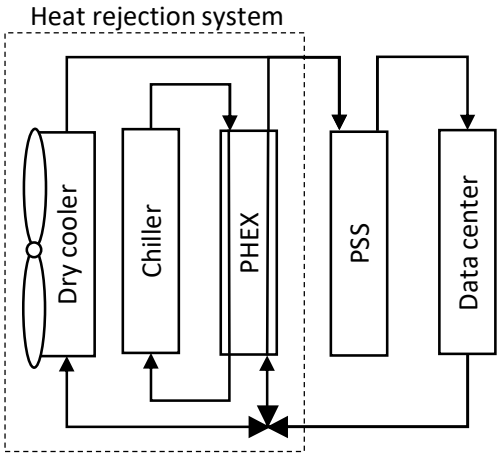

(c)

Figure 6. Configurations of heat rejection system: (a) chiller (MC); (b) indirect free cooling system (IFC); (c) hybrid cooling (IFC + MC)

4.1 Performance metrics

Performance metrics play an important role in operating DCs with high energy-efficiency, reliability, and low total cost of ownership (TOC). Thus, it is vital to obtain the highest computational output from the input energy of DCs. The green grid introduces two metrics (power usage effectiveness (PUE) and water usage effectiveness (WUE)) to measure the energy efficiency of DCs [33]. The PUE is defined as

$$PUE = \frac{P_{Cooling}+P_{Electrical}+P_{IT}}{P_{IT}} \quad (4)$$

where $P_{Cooling}$ is the electrical power consumed by the cooling system. $P_{Electrical}$ includes the power lost in the energy distribution system through line loss and other UPS infrastructure, and the electrical power used to support spaces and light in the DC. P_{IT} denotes the total power consumed by the rack for computing, storage, and network equipment. A low PUE (approaching one) indicates that most of the energy consumed by the DC is used for computing.

The metric called partial power usage effectiveness (PPUE) defines a certain portion of the overall PUE of a DC within a clearly defined boundary. The infrastructure-cooling PPUE is defined as follows:

$$PPUE = \frac{P_{Cooling} + P_{IT}}{P_{IT}} \quad (5)$$

Table 6 shows the active equipment consuming energy on the cooling line-up, which is composed of a SlideIN cooling tower (or two V-shaped dry coolers) and PSS. The $P_{Cooling}$ in $PPUE$ is the sum of the consumptions of the infrastructure cooling equipment.

Element	Quantity during operation	Maximum power	Total maximum power
Dry cooler fans	8	2.88 kW	23.04 kW
Substation pumps	1	2.71 kW	2.71 kW

Table 6. Maximal power consumption of infrastructure cooling system.

WUE is defined as

$$WUE = \frac{Annual\ site\ water\ usage}{P_{IT}} \quad (6)$$

The annual water usage of a site includes the water used for humidification and that evaporated on-site for the energy production or cooling of a DC and its support systems. It is a sustainability metric that measures the amount of water used by DCs to cool IT equipment.

The electrical power consumption of each heat rejection system depends on the external conditions of the DC. It is defined in this study as a function of the external temperature. For example, to provide a reasonable water-return temperature of DC, the speed of the dry cooler fans increases with the external temperature. This increases the power consumption.

The total power consumption under the MC concept is defined as the sum of the power consumption of the substation pumps (one over two) and that of the chiller:

$$P_{MC} = \sum_{i=1}^{m} P_{PSS\ pumps-i} + \sum_{i=1}^{n} P_{Chiller-i} \quad (7)$$

where P is the power consumption. m and n are constants representing the numbers of substation pumps and chillers, respectively, installed in the DC infrastructure. Note that the power consumption of a chiller includes those of its compressor and pumps, which are provided by the manufacturer.

The total power consumption of an IFC cooling system is defined as the sum of the power consumed by the substation pumps, EC pumps, and dry cooler fans:

$$P_{IFC+EC} = \sum_{i=1}^{m} P_{PSS\ pumps-i} + \sum_{i=1}^{o} P_{Dry\ cooler-i} + \sum_{i=1}^{p} P_{EC\ pumps-i} \quad (8)$$

where o and p are constants that represent the numbers of dry coolers and EC pumps, respectively, installed in the DC infrastructure.

The total power consumption of a hybrid cooling mode (MC + IFC) is defined as the sum of the power consumed by the substation pumps, chillers, and dry cooler fans:

$$P_{MC+IFC} = \sum_{i=1}^{m} P_{PSS\ pumps-i} + \sum_{i=1}^{n} P_{Chiller\ -i} + \sum_{i=1}^{o} P_{Dry\ cooler-i} \quad (9)$$

An approach similar to that used in prior studies was adopted for the power consumption of the dry cooler fan [34]. Fan affinity laws indicate that the power consumed by a fan increases cubically with the airflow rate ($\dot{V}$):

$$Fan\ Power \propto (\dot{V})^3 \quad (10)$$

The methodology for calculating the power consumption of the dry cooler is presented in Appendix A (Figure 11). The airflow rate, pressure drop, and outlet air temperature are provided by the manufacturer of the heat exchanger based on the outdoor conditions. This enables the selection of the fan. The power consumption of a fan is determined based on the physical parameters at fan's operating point:

$$P_W = \sum_{i=0}^{3} a_i \dot{v}^i \quad (11)$$

where i and a_i are constants. $\dot{V}$ is the airflow rate (m^3/h) generated by the fans.

The water consumption of the EC used in the IFC system was calculated as a function of the water demand of the EC system using cooling pads. It is determined based on the technical data provided by the manufacturer regarding the airflow rate, external air temperature, and humidity conditions. It is defined as the sum of evaporated water and bleed-off quantities required per hour to operate a dry cooler equipped with an EC system. In addition, WUE can be extracted as the total quantity of water required per kWh. The methodology for calculating WUE is presented in Appendix A (Figure 12).

4.2 Performance analysis under different climatic conditions

The performance of free cooling is affected strongly by the climatic zone [35]. Therefore, four sites worldwide with different climates were investigated for a DC portion of 600 kW: Mumbai (India), Singapore, VintHill (USA), and Roubaix (France). Temperature and relative humidity data of the past 40 years were collected from the weather underground community site [36] and analysed (one record every 30 min). The warmest year in the 40 years for each location was selected. Table 7 shows the selected cities and their average climatic conditions during that year.

City	Elevation (m)	Warmest year	Temperature (°C)		Relative humidity (%)
			Wet bulb	Dry bulb	
Mumbai	14	2018	28.85	23.47	64.64
Singapore	15	2018	28.50	25.25	77.45
VintHill	125	2019	14.35	11.34	73.04
Roubaix	33	2018	11.53	8.80	76.16

Table 7. Average climatic condition during the warmest year in Mumbai, Singapore, VintHill, and Roubaix in the 40 years.

Figure 7(a) shows the temperature frequency in hours per year for the climatic data of each location. The key hours for Mumbai and Singapore are between 25 and 35 °C, whereas these are distributed between -2 °C and 30 °C for VintHill and between 5 and 20 °C for Roubaix.

Figure 7(b), (c), (d), and (e) show the electricity consumption of the DC cooling system with respect to the external temperature of DC in Mumbai, Singapore, VintHill, and Roubaix, respectively, for the three heat rejection systems shown in Figure 6. The results show that the cooling systems require higher levels of cooling in Mumbai (Figure 7(b)) and Singapore (Figure 7(c)) than in VintHill (Figure 7(d)) and Roubaix (Figure 7(e)).

The addition of a dry cooler to the chiller (hybrid mode: MC + IFC) reduced the average electrical consumption by 51.8, 54.8, 82.4, and 92.8 % compared with the MC system, for Mumbai, Singapore, VintHill, and Roubaix, respectively. The MC + IFC system can save energy significantly. Herein, the electricity consumption is limited to dry cooler fans and pumps, whereas the active components of the chiller are idle. Because the IFC system is more directly influenced by the external conditions, the impact of the addition of a dry cooler to the chiller in Roubaix and VintHill (where the outside temperatures are low) is more significant than that observed for Mumbai and Singapore.

The use of an IFC equipped with an EC (IFC + EC) reduces the electrical consumption by 89.5, 89.3, 93.25, and 94.95 % compared with the MC system, for Mumbai, Singapore, VintHill, and Roubaix, respectively. The IFC + EC system shows optimal energy savings. Herein, a reduction in power consumption of at least 89 % could be achieved in all the four locations by restricting the electrical consumption to the dry cooler fans and substation pumps. For Singapore, the water temperature exceeded 27 °C by less than 2 °C. This is reasonable for rack operation under TC-35, as described in Section 3.2.

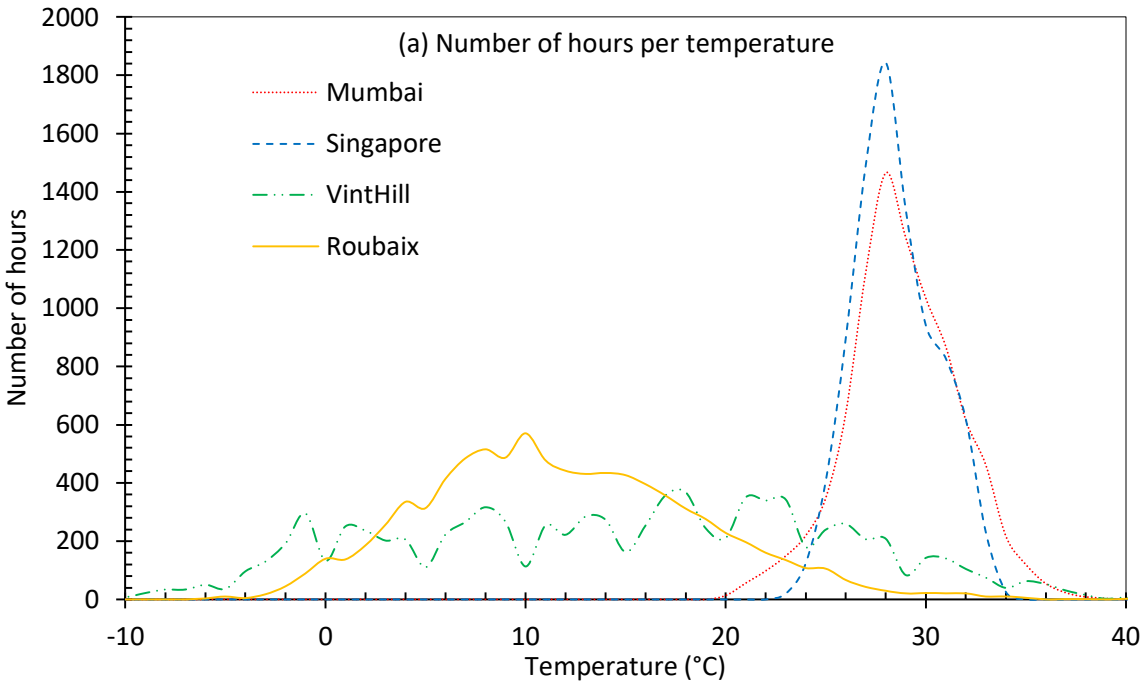

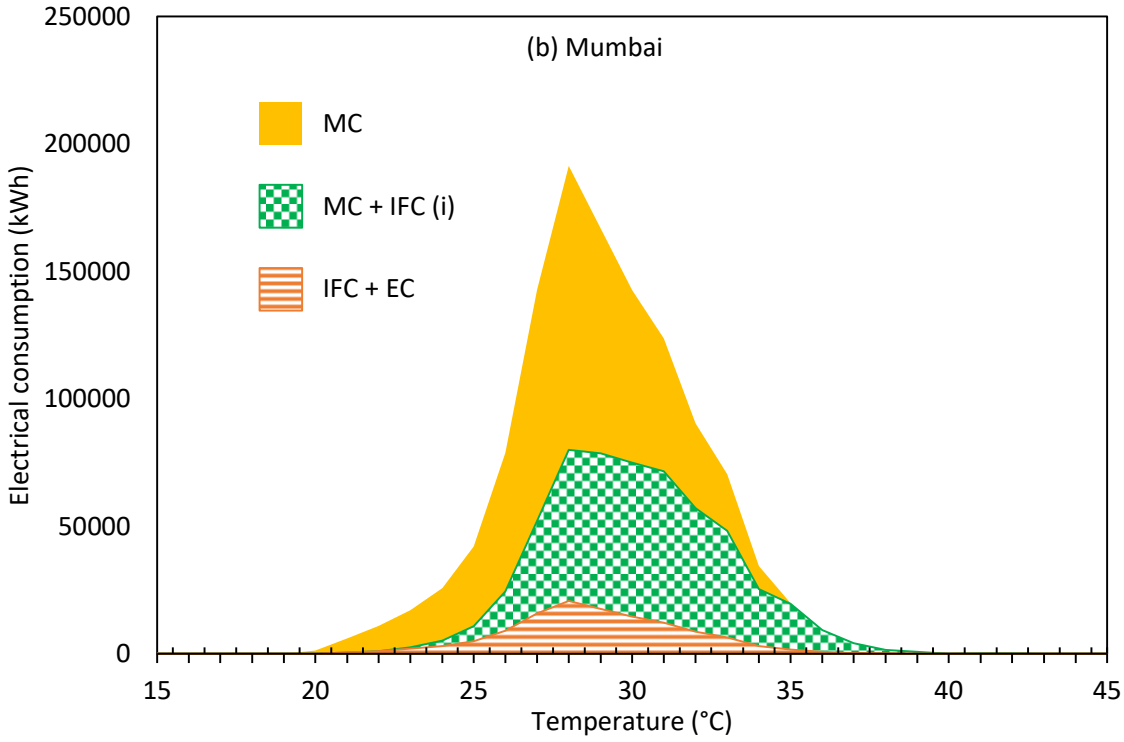
(b) Mumbai
MC
MC + IFC (i)
IFC + EC
Electrical consumption (kWh)
250000
200000
150000
100000
50000
0
15
20
25
30
35
40
45
Temperature (°C)

425

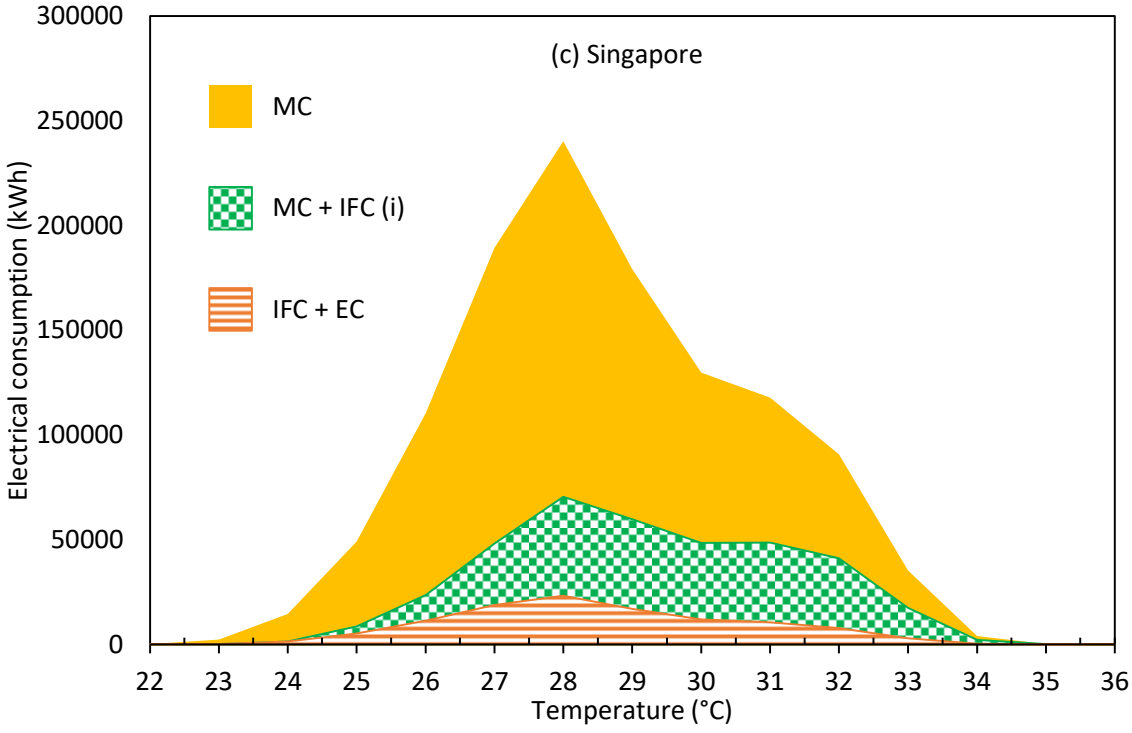
(c) Singapore
MC
MC + IFC (i)
IFC + EC
Electrical consumption (kWh)
300000
250000
200000
150000
100000
50000
0
22
23
24
25
26
27
28
29
30
31
32
33
34
35
36
Temperature (°C)

426

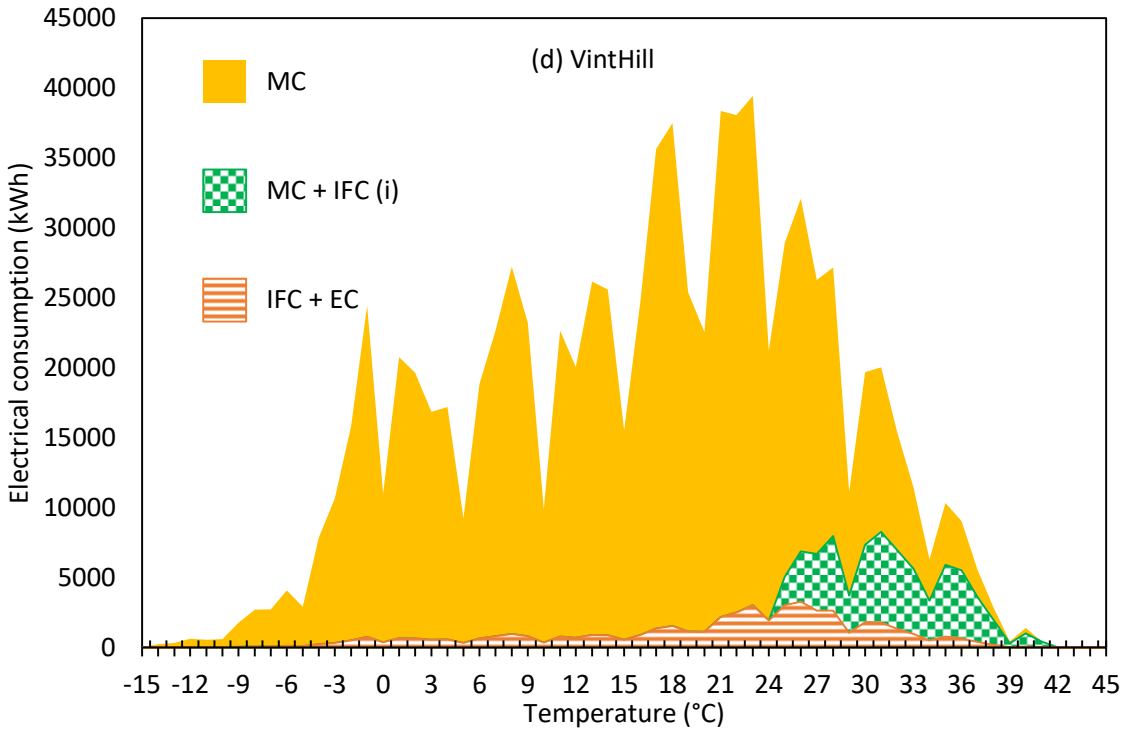
(d) VintHill
MC
MC + IFC (i)
IFC + EC
Electrical consumption (kWh)
45000
40000
35000
30000
25000
20000
15000
10000
5000
0
-15 -12 -9 -6 -3 0 3 6 9 12 15 18 21 24 27 30 33 36 39 42 45
Temperature (°C)

427

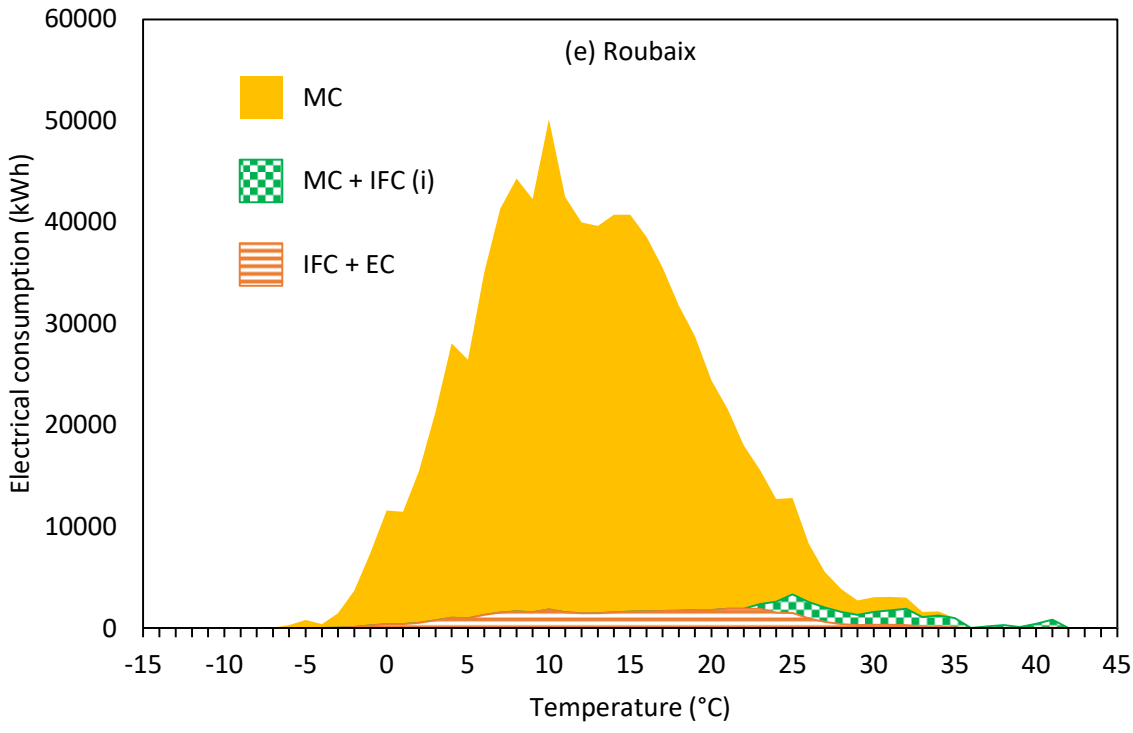
(e) Roubaix
MC
MC + IFC (i)
IFC + EC
Electrical consumption (kWh)
60000
50000
40000
30000
20000
10000
0
-15 -10 -5 0 5 10 15 20 25 30 35 40 45
Temperature (°C)

428

Figure 7. (a) Temperature frequency in hours per year for the cities studied; (b), (c), (d), and (e) annual electricity consumptions of cooling systems of 600 kW DCs under different heat rejection systems in Mumbai, Singapore, VintHill, and Roubaix, respectively.

Figure 8 shows the impact of different cooling systems on the cooling PPUE values at the four locations. The PPUE decreased by 9.6, 10, 12, and 12.5 % with respect to the MC system for Mumbai, Singapore, VintHill, and Roubaix, respectively, when the hybrid system was used. Moreover, it decreased by 16.4, 16.2, 13.6, and 12.8 % for Mumbai, Singapore, VintHill, and Roubaix, respectively, when the IFC + EC system was used.

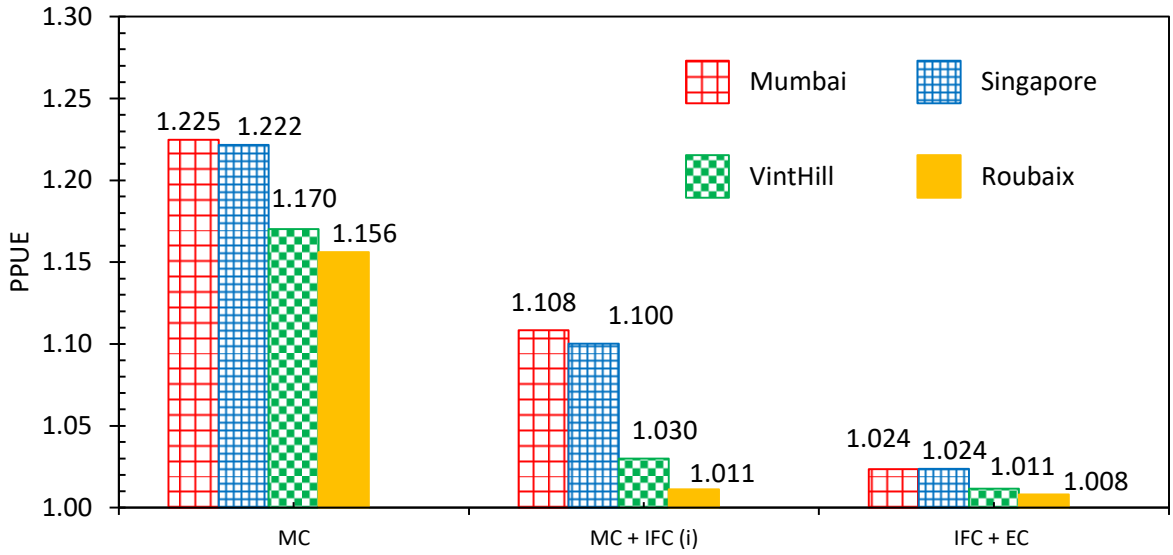

Figure 8. DC cooling PPUE under different cooling heat rejection systems.

5. Impact of water temperature profile

5.1 Effect of temperature difference of rack

By using the IFC + EC system with a DC temperature difference of 20 K rather than 15 K (Figure 3), the PPUE values were reduced by approximately 0.3, 0.3, 0.2, and 0.1% and the WUE values by approximately 42, 38, 49, and 61 % for Mumbai, Singapore, VintHill, and Roubaix, respectively (see Figure 9(a) and (b)). This is related to the use of the EC system to a lesser extent when the temperature difference is 20 K because the EC is on when the outdoor temperature is higher than 26 °C (rather than 24 °C) for the case of 15 K.

5.2 Effect of increasing DC water inlet temperature

The impact of the increase in the temperature of water supplied to the DC by 5 K on the DC performance is analysed in this section. This is because it enhances the dry cooler performance and reduces the DC PPUE and WUE. However, it would increase the ambient air temperature and WB inlet temperature of the racks, as shown in Table 8.

Temperature (°C)	DC Temperature Profile	
	ΔT = 20 K	ΔT = 20 K + 5 K
T_{Rack-i}	27	33
T_{RDHX_air-o}	30	35
T_{RDHX-o}	35	40
T_{WC-i}	45	50
T_{WC-o}	50	55
T_{Rack-o}	47	52

Table 8. 20 K + 5 K cooling system topology.

Figure 9(c) and (d) shows the cooling PPUE and WUE, respectively, for the four locations with IFC + EC, a temperature difference of 20 K, and an increase in the temperature of DC supply-water by 5 K. An increase in the temperature of supplied water by 5 K resulted in a reduction in PPUE values by 0.4, 0.5, 0.2, and 0.2 % and in WUE values by 38, 37, 30, and 56 % for Mumbai, Singapore, VintHill, and Roubaix, respectively, compared with the case of 20 K presented in the previous section. An increase in the temperature of supplied water by 5 K implies a shift in the EC system water supply by 5 K. That is, the EC system would be activated at 29 °C rather than 26 °C (for the 20 K case). Furthermore, this increment in water inlet temperature of DC could be handled by all the racks under TC-35 (as described in Section 3.2).

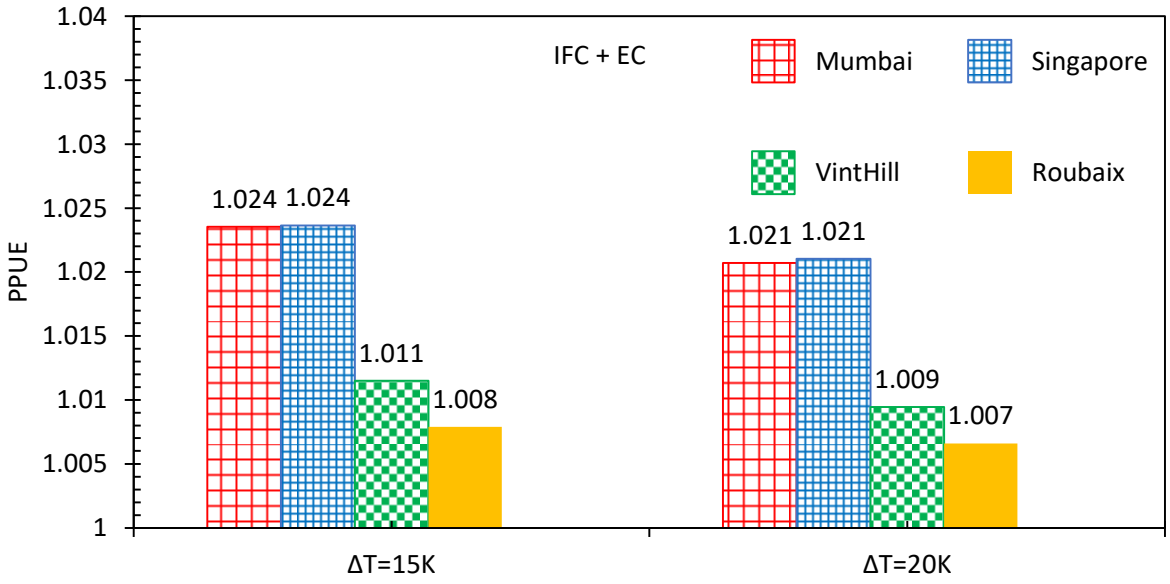
IFC + EC
Mumbai
Singapore
VintHill
Roubaix
PPUE
1.04
1.035
1.03
1.025
1.02
1.015
1.01
1.005
1
1.024
1.024
1.011
1.008
1.021
1.021
1.009
1.007
ΔT=15K
ΔT=20K

(a)

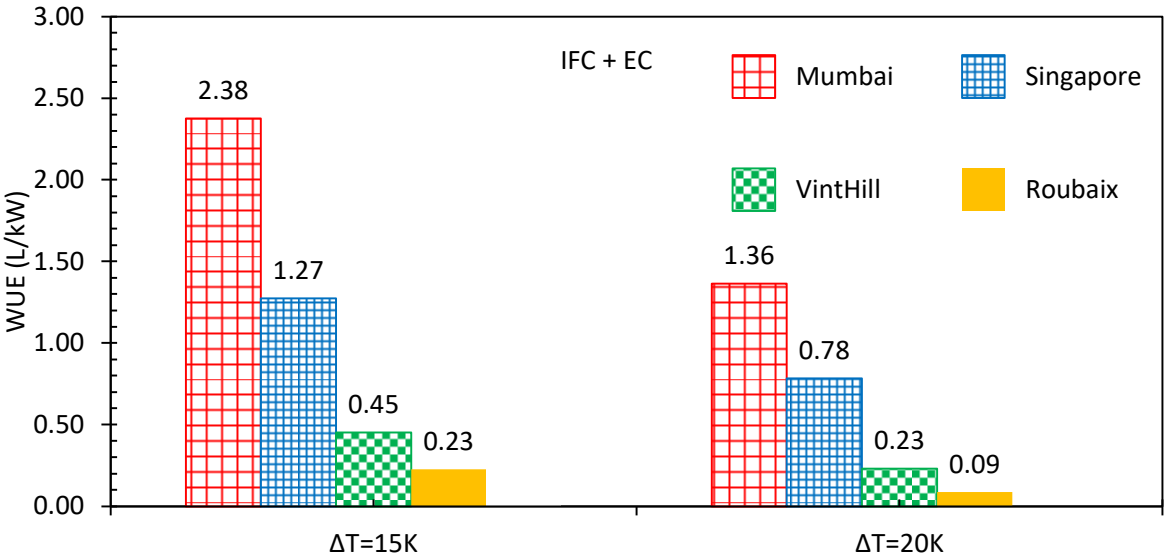
IFC + EC
Mumbai
Singapore
VintHill
Roubaix
WUE (L/kW)
3.00
2.50
2.00
1.50
1.00
0.50
0.00
2.38
1.27
0.45
0.23
1.36
0.78
0.23
0.09
ΔT=15K
ΔT=20K

(b)

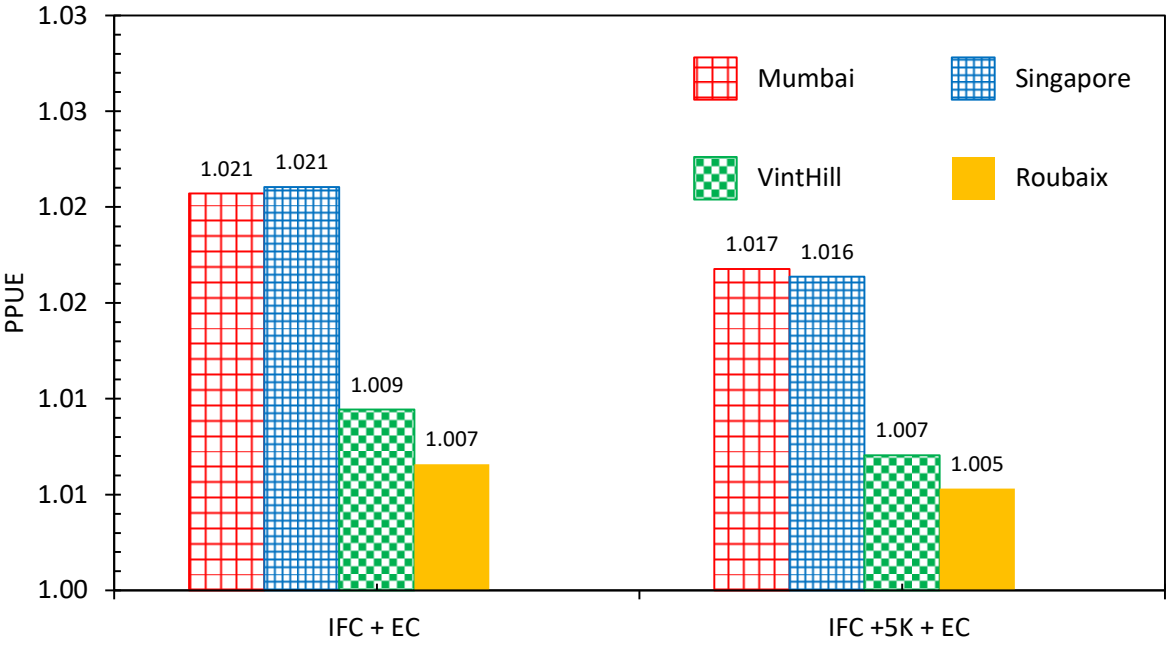

(c)

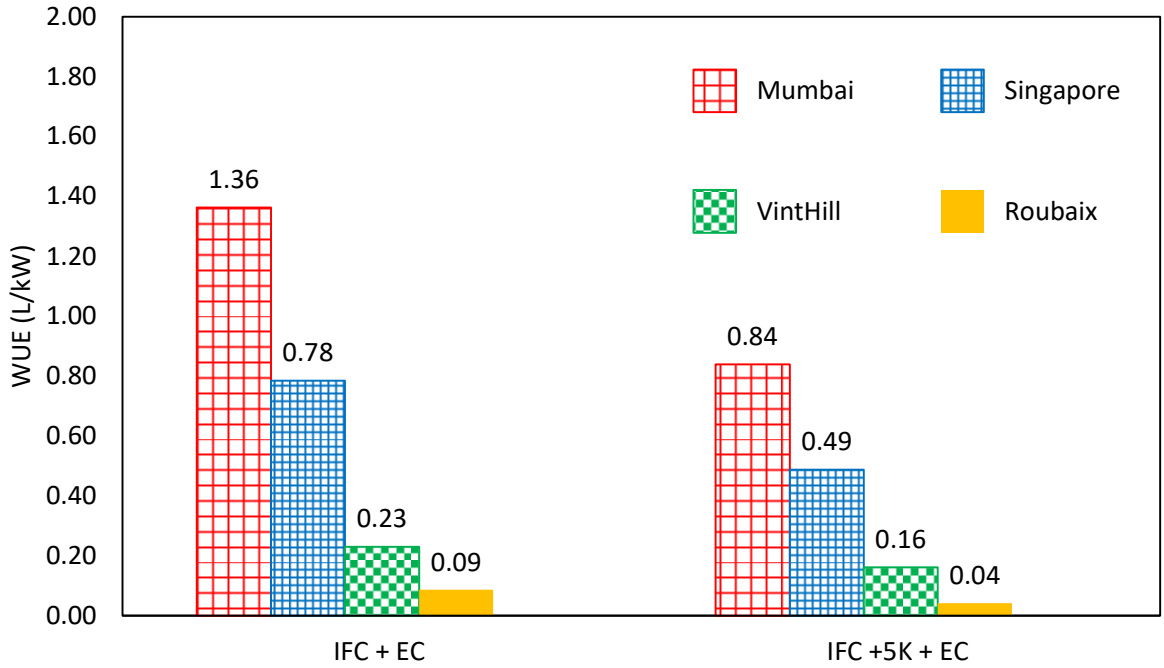

(d)

Figure 9. (a) Cooling PPUE under temperature differences of 15 K and 20 K; (b) WUE under temperature differences of 15 K and 20 K; (c) Cooling PPUE when the temperature of water supplied to DC increases by 5 K under 20 K; (d) WUE when the temperature of water supplied to DC increases by 5 K under 20 K.

The water consumption of DCs has global and regional impacts on ecosystems (e.g., on river flow and groundwater levels). This, in turn, may influence the overall water resources of a territory in the context of water scarcity. Thus, it is vital to reduce the WUE values of DCs, which affect the annual water consumption of DCs. Figure 10 shows a comparison of the annual water consumption of a 600 kW DC for different climatic conditions with an increase in the temperature of water supplied to DC by 5 K under a temperature difference of 20 K. For example, an increase in the supplied-water temperature by 5 K caused a reduction in the annual water consumption from 7160 m^3 to 4406 m^3 (62%) for Mumbai city and from 452 m^3 to 214 m^3 (47%) for Roubaix.

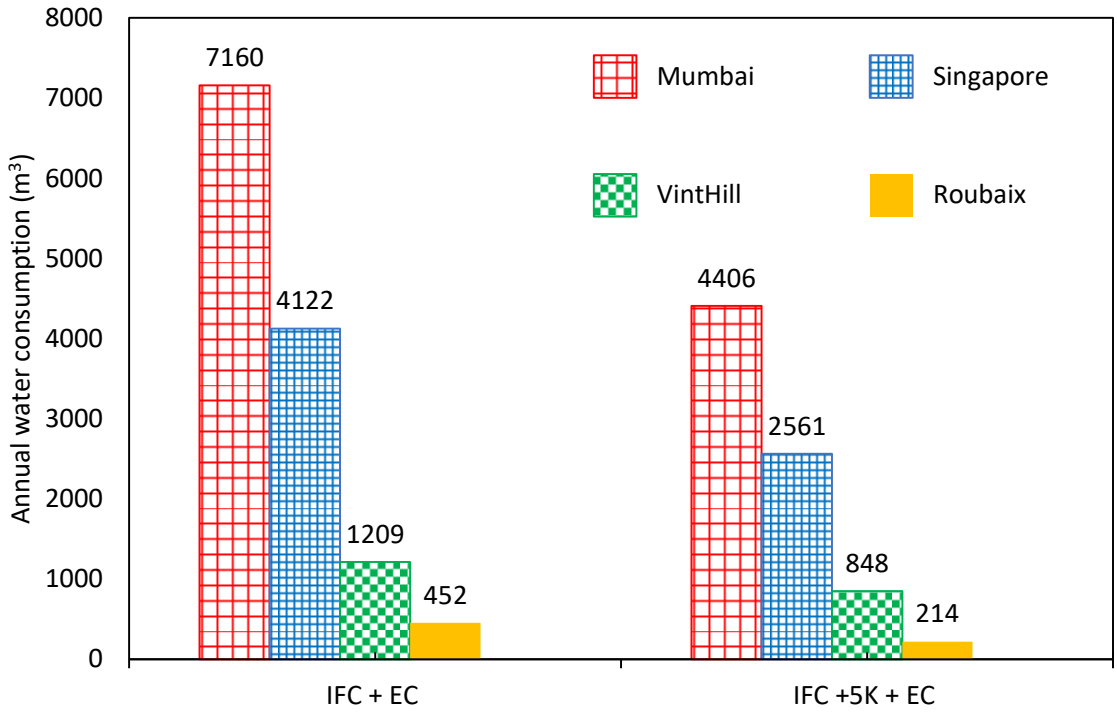

Figure 10. Comparison of annual water consumption by 600 KW DC for different climatic conditions with an increase in the temperature of water supplied to DC by 5 K under a temperature difference of 20 K.

The previous results are summarised in Table 9. It shows the variation in PPUE under different climatic conditions and for different cooling systems and temperature profiles. The improvements in WUE for the IFC + EC system are shown in Table 10.

Cases			Sites			
			Mumbai	Singapore	VintHill	Roubaix
			PPUE			
Case 1	MC	-	1.225	1.222	1.170	1.156
Case 2	MC + IFC	-	1.108	1.100	1.030	1.011
Case 3	IFC + EC	dT = 15 K	1.024	1.024	1.011	1.008
Case 4	IFC + EC	dT = 20 K	1.021	1.021	1.009	1.007
Case 5	IFC + EC	dT = 20 K + 5 K	1.017	1.016	1.007	1.006

Table 9. PUE values under different climatic conditions and for different cooling systems and temperature profiles

dT	Sites			
	Mumbai	Singapore	VintHill	Roubaix
	WUE (l/kWh)			
15 K	2.38	1.27	0.45	0.23
20 K	1.36	0.78	0.23	0.09
20 K + 5 K	0.84	0.49	0.16	0.04

Table 10. WUE values for improvements in IFC + EC system.

6. Conclusion

This paper presents a new cooling topology for information technology racks based on liquid cooling deployed within OVHcloud data centres. Within this topology, the rack-cooling system is based on a combination of close-coupled cooling and direct-to-chip cooling. An experimental investigation was conducted at the rack level to validate the direct impact of temperature difference (15 K and 20 K) on operational information-technology racks under thermal conditions of 27 and 35 °C. Five racks with operational servers were tested. A temperature difference was validated for all the IT racks. The 20 K temperature-difference profile was validated under the two thermal conditions with the proposed rear-door heat exchanger configuration.

The impact of these temperature difference profiles (15 K and 20 K) on the data-centre performance was analysed using three heat rejection systems (a mechanical cooling system using chillers, indirect free cooling, and hybrid chillers with integrated intelligent dry coolers) under four climatic conditions for a data centre of 600 kW. Our results can be summarized as follows:

- Adding a dry cooler to the chiller (hybrid mode) reduced the average electrical consumption by at least 52 % compared with the mechanical cooling system in all the four locations (Mumbai, Singapore, VintHill, and Roubaix).
- Indirect free cooling equipped with an evaporative cooling system showed optimal energy savings (a reduction in annual power consumption of at least 89 % compared with the mechanical cooling system). The cooling partial power usage effectiveness also reduced (by at least 16 %) compared with that of the mechanical cooling system.

The impact of the water temperature profile on the partial power usage effectiveness and water usage effectiveness of data centre was analysed to optimise the indirect free cooling system equipped with an evaporative cooling system through two approaches: rack temperature difference and by increasing the water inlet temperature of the data centre.

- Increasing the temperature difference of the racks from 15 K to 20 K significantly reduced the water usage effectiveness and marginally reduced the partial power usage effectiveness (by approximately 40 % and 0.1 %, respectively).

- Increasing the temperature of cold facility water supplied to data centre by 5 K under the 20 K temperature-difference profile significantly reduced the water usage effectiveness and marginally reduced the partial power usage effectiveness (by approximately 38 % and 0.1 %, respectively).

With reference to the high return water temperature (which exceeds 50 °C), the application of this liquid-cooled data centre topology enables the use of the waste heat of IT equipment for other applications such as domestic hot water, network heating, and industrial applications.

Many investigations could be conducted in future work, such as hybrid liquid cooling by integrating water cooling with a dielectric fluid (which has a higher thermal conductivity than air). In addition, the footprint (kW/m²), capital expenditure, operating expenditure, and energy at the data-centre level can be analysed.

Appendix A

Appendix A provides detailed information on the locations of temperature, pressure, differential pressure, and flow-rate sensor measurement and the names of the sensors for the climatic chamber test bench (see Figure 4). In addition, it provides detailed information on the methodologies for calculating power consumption and WUE (see Figures 10 and 11, respectively).

Figure 4 (d) shows the climatic chamber test bench. The air temperature sensors, wall temperature sensors, and water temperature sensors are illustrated in green, blue, and orange, respectively. A thermocouple that measures air temperature was installed on each console suction port. Three thermocouples each were installed on the inlet and outlet of each RDHX to measure the hot air and cold air temperatures, respectively. With regard to the air cooling circuit (AC), two immersed thermocouples were installed on the rack's inlet and outlet manifolds to measure the water temperature. A thermocouple was installed at each RDHX outlet to measure the water temperature. A thermocouple was installed at the AC outlet to measure the temperature of the water entering the PHEXs of the CDU. For the water cooling circuit (WC), two thermocouples were installed on the water block inlet and outlet manifolds to measure the water temperature. Two Kobold [37] 5–90 l/min flow-rate sensors were installed in the AC and WC circuits to measure the flow rate of the water fed to the rack and its WBs, respectively. Two 0–6 bar Kobold pressure sensors were installed on the inlet and outlet of the rack. A 0–6 bar Kobold pressure sensor was installed at the inlet of the CDU PHEXs (AC circuit) to measure the water pressure after the RDHXs. Two 0-6 bar Kobold pressure sensors were installed on the WC inlet and outlet manifolds. Two Kobold differential pressure sensors (3.73–373 mbar) were installed on the AC circuits to measure the pressure drop of the RDHXs and the total pressure drop of the rack. Moreover, a Kobold differential pressure sensor was installed on the WC circuits to measure the overall pressure drop of the CDUs.

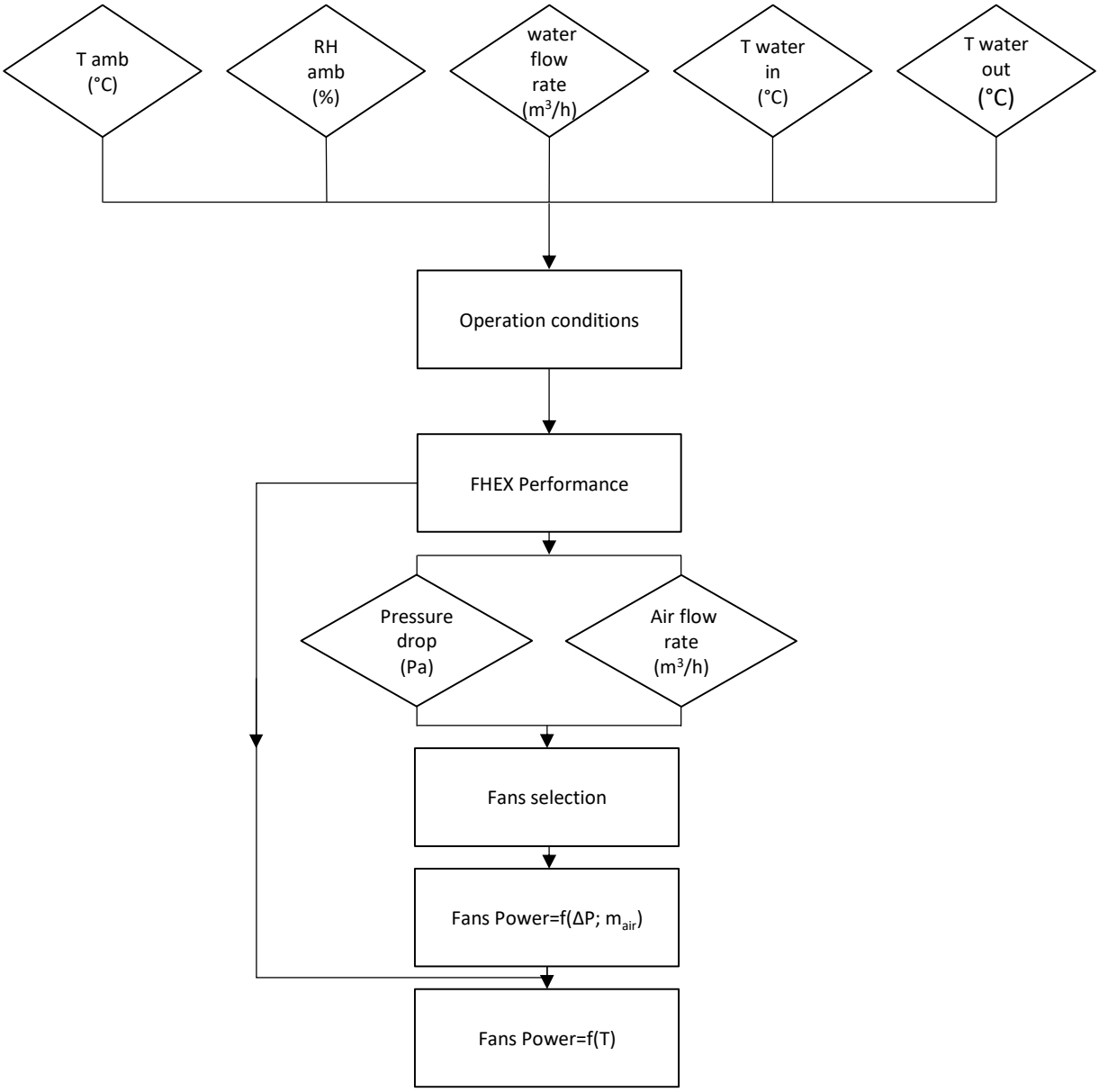

563

564 Figure 11. Methodology for calculating power consumption.

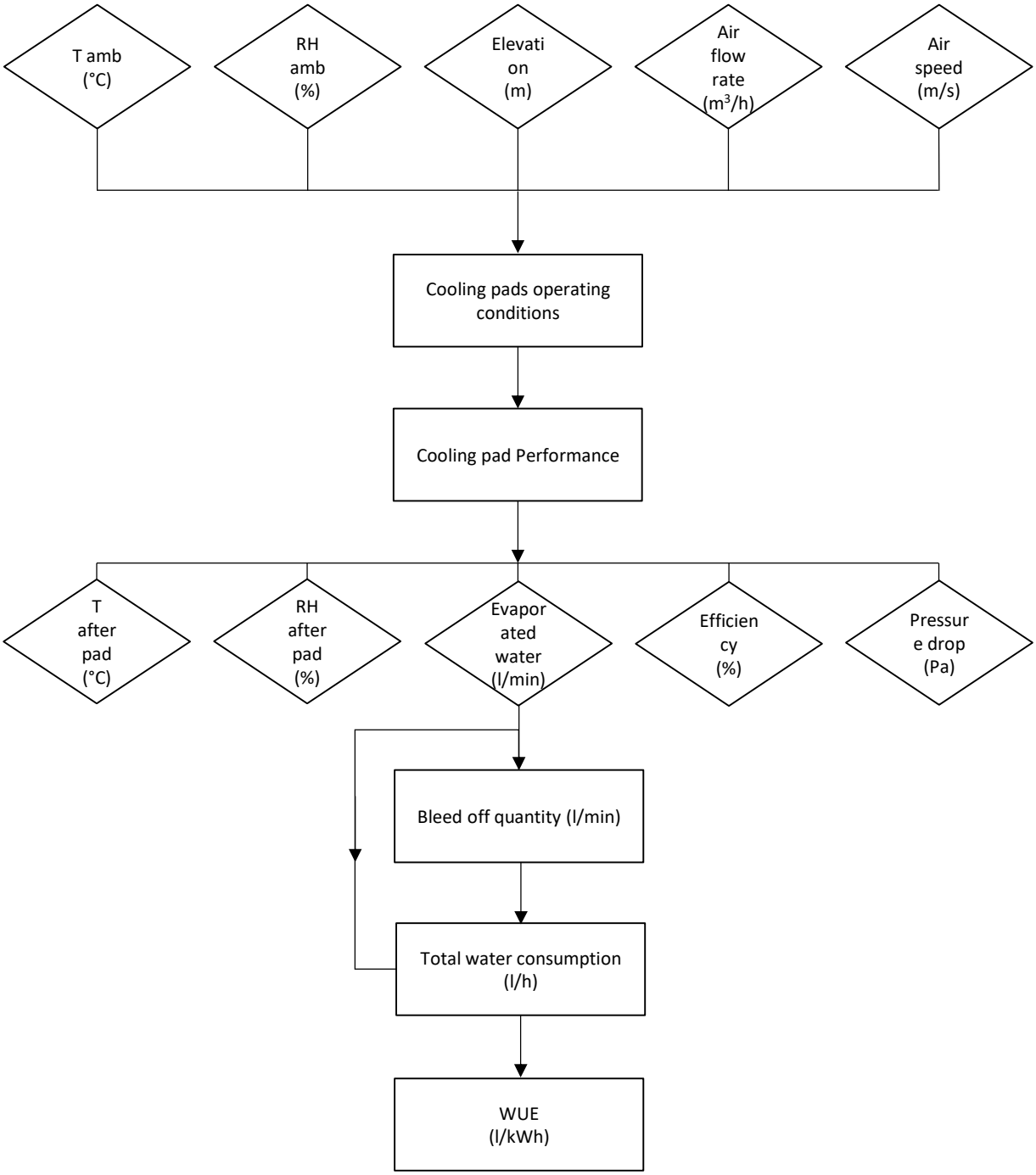

Figure 12. Methodology for calculating WUE.

Acknowledgement

The authors of this article wish to thank the OVHcloud R&D-Cooling team for their help during concept development, test bench design, and the test.

Nomenclature

General Nomenclature		Greek symbols and subscripts	
AC	Air Cooling	*Δ*	Increment, deviation
WUE	Water Usage Effectiveness	*Σ*	Sum
CDU	Cooling Distribution Unit	η	Efficiency
PSS	Pumping Substation	*A*	Constant
DC	Data Centre	*B*	Constant
DSI	Direct Steam Injection	*C*	Constant
FHEX	Finned Heat Exchanger	*I*	Inlet, index
IFC	Indirect Free Cooling	*M*	Constant
IT	Information Technology	*N*	Constant
$\dot{m}$	Mass flow rate (kg/s)	*O*	Outlet, constant
MC	Mechanical Cooling	*P*	Constant
P	Electric power (W), Pressure (Pa)	*X*	Constant
PHEX	Plate Heat Exchanger	*Y*	Constant
PUE	Power Usage Effectiveness	*Z*	Constant
PPUE	Partial Power Usage Effectiveness		
Q	Heat load (W)		
EC	Evaporative Cooling		
RDHX	Rear-Door Heat Exchanger		
T	Temperature (°C)		
TC	Thermal Conditions		
WB	Water Block		
WC	Water Cooling		

7. References

[1] R. Buyya, C. Vecchiola, S.T. Selvi, Mastering cloud computing: foundations and applications programming, Morgan Kaufmann, Amsterdam ; Boston, 2013.

[2] Data centres and energy – from global headlines to local headaches? – Analysis, IEA. (n.d.). https://www.iea.org/commentaries/data-centres-and-energy-from-global-headlines-to-local-headaches (accessed April 4, 2022).

[3] P. Johnson, T. Marker, Prepared for Equipment Energy Efficiency Committee (E3), (n.d.) 28.

[4] S. Alkharabsheh, J. Fernandes, B. Gebrehiwot, D. Agonafer, K. Ghose, A. Ortega, Y. Joshi, B. Sammakia, A Brief Overview of Recent Developments in Thermal Management in Data Centers, Journal of Electronic Packaging. 137 (2015) 040801. https://doi.org/10.1115/1.4031326.

[5] Q. Zhang, Z. Meng, X. Hong, Y. Zhan, J. Liu, J. Dong, T. Bai, J. Niu, M.J. Deen, A survey on data center cooling systems: Technology, power consumption modeling and control strategy optimization, Journal of Systems Architecture. 119 (2021) 102253. https://doi.org/10.1016/j.sysarc.2021.102253.

[6] E. Oró, A. Garcia, J. Salom, Experimental and numerical analysis of the air management in a data centre in Spain, Energy and Buildings. 116 (2016) 553–561. https://doi.org/10.1016/j.enbuild.2016.01.037.

[7] S.A. Nada, M.A. Said, M.A. Rady, CFD investigations of data centers' thermal performance for different configurations of CRACs units and aisles separation, Alexandria Engineering Journal. 55 (2016) 959–971. https://doi.org/10.1016/j.aej.2016.02.025.

[8] J. Dai, M.M. Ohadi, D. Das, M.G. Pecht, Optimum Cooling of Data Centers, Springer New York, New York, NY, 2014. https://doi.org/10.1007/978-1-4614-5602-5.

[9] Y. Fulpagare, A. Bhargav, Advances in data center thermal management, Renewable and Sustainable Energy Reviews. 43 (2015) 981–996. https://doi.org/10.1016/j.rser.2014.11.056.

[10] S. Zimmermann, I. Meijer, M.K. Tiwari, S. Paredes, B. Michel, D. Poulikakos, Aquasar: A hot water cooled data center with direct energy reuse, Energy. 43 (2012) 237–245. https://doi.org/10.1016/j.energy.2012.04.037.

[11] V. Ljungdahl, M. Jradi, C. Veje, A decision support model for waste heat recovery systems design in Data Center and High-Performance Computing clusters utilizing liquid cooling and Phase Change Materials, Applied Thermal Engineering. 201 (2022) 117671. https://doi.org/10.1016/j.applthermaleng.2021.117671.

[12] H. Coles, S. Greenberg, Direct Liquid Cooling for Electronic Equipment, 2014. https://doi.org/10.2172/1134242.

[13] H. Moazamigoodarzi, S. Pal, D. Down, M. Esmalifalak, I.K. Puri, Performance of a rack mountable cooling unit in an IT server enclosure, Thermal Science and Engineering Progress. 17 (2020) 100395. https://doi.org/10.1016/j.tsep.2019.100395.

[14] K. Nemati, H.A. Alissa, U. Puvvadi, B.T. Murray, B. Sammakia, K. Ghose, Experimental characterization of a Rear Door Heat exchanger with localized containment, in: 2016 15th IEEE Intersociety Conference on Thermal and Thermomechanical Phenomena in Electronic Systems (ITherm), IEEE, Las Vegas, NV, USA, 2016: pp. 710–719. https://doi.org/10.1109/ITHERM.2016.7517617.

[15] A. Almoli, A. Thompson, N. Kapur, J. Summers, H. Thompson, G. Hannah, Computational fluid dynamic investigation of liquid rack cooling in data centres, Applied Energy. 89 (2012) 150–155. https://doi.org/10.1016/j.apenergy.2011.02.003.

[16] O.S. Osman, R.M. El-Zoheiry, M. Elsharnoby, S.A. Nada, Performance enhancement and comprehensive experimental comparative study of cold plate cooling of electronic servers using different configurations of mini-channels flow, Alexandria Engineering Journal. 60 (2021) 4451–4459. https://doi.org/10.1016/j.aej.2021.03.027.

[17] Y. Zhang, Y. Zhao, S. Dai, B. Nie, H. Ma, J. Li, Q. Miao, Y. Jin, L. Tan, Y. Ding, Cooling technologies for data centres and telecommunication base stations – A comprehensive review, Journal of Cleaner Production. 334 (2022) 130280. https://doi.org/10.1016/j.jclepro.2021.130280.

[18] R. Udakeri, V. Mulay, D. Agonafer, Comparison of Overhead Supply and Underfloor Supply with Rear Heat Exchanger in High Density Data Center Clusters, in: 2008 Twenty-Fourth Annual IEEE Semiconductor Thermal Measurement and Management Symposium, IEEE, San Jose, CA, 2008: pp. 165–172. https://doi.org/10.1109/STHERM.2008.4509385.

[19] A. Carbó, E. Oró, J. Salom, M. Canuto, M. Macías, J. Guitart, Experimental and numerical analysis for potential heat reuse in liquid cooled data centres, Energy Conversion and Management. 112 (2016) 135–145. https://doi.org/10.1016/j.enconman.2016.01.003.

[20] K.-P. Lee, H.-L. Chen, Analysis of energy saving potential of air-side free cooling for data centers in worldwide climate zones, Energy and Buildings. 64 (2013) 103–112. https://doi.org/10.1016/j.enbuild.2013.04.013.

[21] Y. Udagawa, S. Waragai, M. Yanagi, W. Fukumitsu, Study on free cooling systems for data centers in Japan, in: Intelec 2010, IEEE, Orlando, FL, USA, 2010: pp. 1–5. https://doi.org/10.1109/INTLEC.2010.5525676.

[22] Y. Zhang, Z. Wei, M. Zhang, Free cooling technologies for data centers: energy saving mechanism and applications, Energy Procedia. 143 (2017) 410–415. https://doi.org/10.1016/j.egypro.2017.12.703.

[23] T. Malkamäki, S.J. Ovaska, Solar Energy and Free Cooling Potential in European Data Centers, Procedia Computer Science. 10 (2012) 1004–1009. https://doi.org/10.1016/j.procs.2012.06.138.

[24] S. Shao, H. Liu, H. Zhang, C. Tian, Experimental investigation on a loop thermosyphon with evaporative condenser for free cooling of data centers, Energy. 185 (2019) 829–836. https://doi.org/10.1016/j.energy.2019.07.095.

[25] C. Liao, S. Singh, T. Wang, Characterizing the performance of alternative evaporative cooling pad media in thermal environmental control applications, Journal of Environmental Science and Health, Part A. 33 (1998) 1391–1417. https://doi.org/10.1080/10934529809376795.

[26] H.M. Daraghmeh, C.-C. Wang, A review of current status of free cooling in datacenters, Applied Thermal Engineering. 114 (2017) 1224–1239. https://doi.org/10.1016/j.applthermaleng.2016.10.093.

[27] ASHRAE Handbook—HVAC Systems and Equipment (SI), CHAPTER 22 HUMIDIFIERS.pdf, (n.d.).

[28] Q. Chen, N. Pan, Z.-Y. Guo, A new approach to analysis and optimization of evaporative cooling system II: Applications, Energy. 36 (2011) 2890–2898. https://doi.org/10.1016/j.energy.2011.02.031.

[29] D.A. Warke, S.J. Deshmukh, Experimental Analysis of Cellulose Cooling Pads Used in Evaporative Coolers, (n.d.) 8.

[30] ebm-papst France - ebm-papst - World market leader for energy-saving fans and motors, (n.d.). https://www.ebmpapst.fr/fr/ (accessed April 4, 2022).

[31] R.J. Moffat, Describing the uncertainties in experimental results, Experimental Thermal and Fluid Science. 1 (1988) 3–17. https://doi.org/10.1016/0894-1777(88)90043-X.

[32] National Instruments, (n.d.). https://www.ni.com/fr-fr.html (accessed April 4, 2022).

[33] E. Jaureguialzo, PUE: The Green Grid metric for evaluating the energy efficiency in DC (Data Center). Measurement method using the power demand, in: 2011 IEEE 33rd International Telecommunications Energy Conference (INTELEC), IEEE, Amsterdam, Netherlands, 2011: pp. 1–8. https://doi.org/10.1109/INTLEC.2011.6099718.

[34] S. Yeo, H.-H.S. Lee, SimWare: A Holistic Warehouse-Scale Computer Simulator, (n.d.) 8.

[35] K. Zhang, Y. Zhang, J. Liu, X. Niu, Recent advancements on thermal management and evaluation for data centers, Applied Thermal Engineering. 142 (2018) 215–231. https://doi.org/10.1016/j.applthermaleng.2018.07.004.

[36] Local Weather Forecast, News and Conditions | Weather Underground, (n.d.). https://www.wunderground.com/ (accessed April 4, 2022).

[37] K.M. GmbH, La mesure industrielle et de contrôle dans le domaine de l'écoulement, pression, niveau et température | Kobold Messring GmbH, (n.d.). https://www.kobold.com/fr (accessed April 4, 2022).

Performance analysis of new liquid cooling topology and its impact on data centres

New liquid cooling topology
Combination of close coupled cooling and direct to chip cooling

Rack's investigation

Performance Analysis on a DC of 600kW

Experimental setup

- Five IT racks with operational servers are tested
- Under two temperature profiles: 15 K and 20 K
- Under Two thermal conditions TC-27 and TC-35 °C

Numerical calculation

- Three heat rejection systems are compared
- Three DC temperature profiles
- Four different climatic locations
- PPUE comparison
- WUE comparison

Dry cooler

Pumping substation

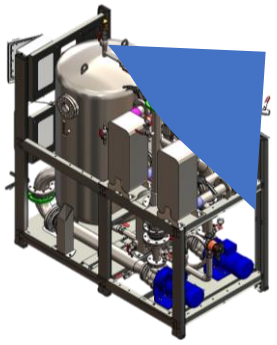

IT Rack

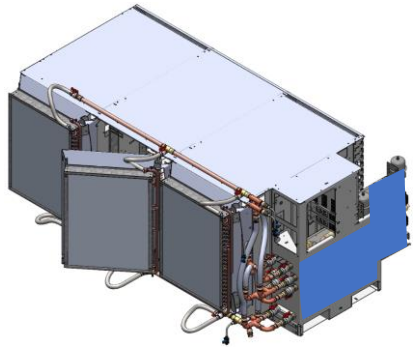

Liquid cooled server

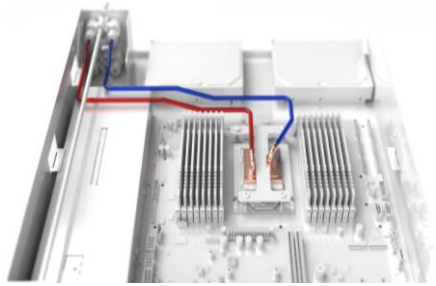

DC cooling infrastructure

m | dm

Rack cooling system

cm | mm

89%

Saving in Electrical consumption

IFC vs MC

16%

Improvement in PPUE

IFC vs MC

60%

Enhancement in WUE

20K+5K vs 15K